CDF/PHYS/EXOTIC/PUBLIC/8360
Version 0.001
July 26, 2006

Search for Lepton-Photon +X events in $929 pb^{-1}$

Preliminary

DRAFT!

Andrei Loginov
Institute for Theoretical and Experimental Physics,
Moscow, Russia
Henry Frisch
Enrico Fermi Institute, University of Chicago
Chicago, IL 60637

Abstract

We have updated the search for the anomalous production of events with a high E_T photon and a high E_T electron or muon described in CDF7550 by adding data taken up to the March 2006 shutdown. The search includes measurements of the production of events with additional high E_T leptons, photons, missing transverse energy ($\not\!\!E_{\mathrm{T}}$), or total transverse energy. The kinematic selection criteria search are the same as in the CDF Run I search so that the present search is *à priori*. The total luminosity now is 929 pb^{-1}, a factor of 3 larger than that described in CDF7550. The analysis itself is unchanged. We describe a small number of changes to the detector in the new data, the new datasets, and control samples and validation.

We find 163 $\ell\gamma\not\!\!E_{\mathrm{T}}$ events versus a Standard Model expectation of $148.07 \pm 5.10(stat) \pm 11.93(sys)$. The 163 events consist of 96 events in the $e\gamma$ channel and 67 events in the $\mu\gamma$ channel, versus expectations of $94.17 \pm 4.71(stat) \pm 6.64(sys)$ and $53.90 \pm 1.94(stat) \pm 6.84(sys)$) events, respectively.

The Run I search was motivated by a single event with two electrons, two photons, and $\not\!\!E_{\mathrm{T}}$. We find 0 multigamma+lepton events in the much larger Run II sample. There are 74 multilepton+gamma events, versus an expectation of $64.93 \pm 0.89(stat) \pm 7.60(sys)$ events. These consist of 53 and 21 events, versus expectations of $38.95 \pm 0.71(stat) \pm 4.75(sys)$ and $25.95 \pm 0.56(stat) \pm 3.04(sys)$ events, respectively.

We observe no $\ell\gamma\gamma$ or $e\mu\gamma$ events, versus the expectation of $0.62 \pm 0.15(tot)$ and $1.01 \pm 0.33(tot)$ events, respectively.

Contents

1 Introduction

We have updated the lepton-gamma+X search [1] for the full data-set up to the March 2006 shutdown. The total luminosity for the search is now 929 fb^{-1}.

This note is intended to be read as an incremental update of the analysis of $305pb^{-1}$ described in CDF7550 [2]; rather than describe everything over again in detail, we will describe only things that are different from the CDF7550 description. The intent has been to make no changes in the analysis, so that the new data (0h and 0i datasets), which is 2/3 of the total, is analyzed with exactly the same cuts and techniques of the first 1/3 (0d datasets). Consequently the changes described here are almost completely in the sections dealing with data. If some description of something that you would like to know about is not in this note, please go to CDF7550 for a detailed description – the something hasn't changed.

2 Datasets and MC Samples

The data used for this analysis consists of $929pb^{-1}$ end of 2004 and the March 2006 shutdown.

As in Run I, the muon-photon samples are taken from a logical 'OR' of the inclusive high-P_T muon sample (*bhmu0d, bhmu0h, bhmu0i*) and the inclusive high-P_T photon sample (*cph10d, cph10h, cph10i*); this was done to ensure a high and stable trigger efficiency for muons. For consistency, electron-photon candidates are also obtained from a logical 'OR' of the inclusive high-P_T electron sample, *bhel0d, bhel0h, bhel0i*, and the inclusive high-P_T photon sample (*cph10d, cph10h, cph10i*). Each of these samples was ntupled using the UC flat ntuple [3, 4]. We use good run list v13, including recovered runs. We require bits (1,1,1,1).

We use MadGraph and Baur 5.3.3 MC ($Z\gamma$, $W\gamma$, $Z\gamma\gamma$, $W\gamma\gamma$) [2, 5, 6].

We check scale factors/trigger efficiencies we are using by plotting $Z^0 \to e^+e^-$ and $Z^0 \to \mu^+\mu^-$ invariant masses in DATA and MC (Figure 1)

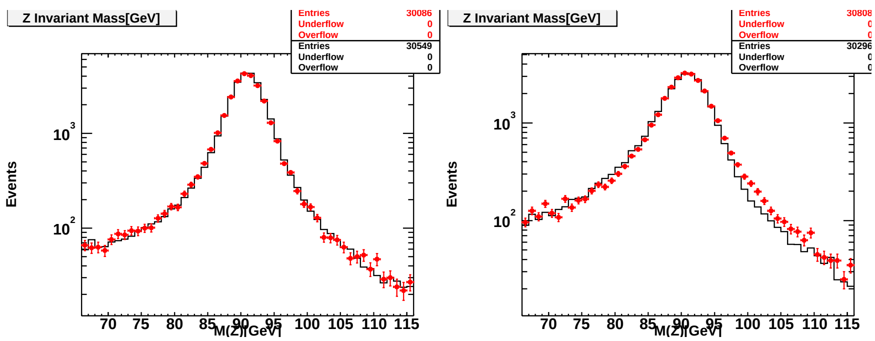

Figure 1: The $Z^0 \to e^+e^-$ (on the left) and $Z^0 \to \mu^+\mu^-$ (on the right) control samples 'sanity-check' plots. The histogram is the prediction from the $Z^0 \to e^+e^-$ and $Z^0 \to \mu^+\mu^-$ MC samples (ztop2i and ztop0i); the points are the $Z^0 \to e^+e^-$ ($Z^0 \to \mu^+\mu^-$) candidates from the data. Background estimates are not included.

3 Background Estimates

We summarize our background estimates in thie section.

- Diboson and triboson production
  - Baur and MadGraph $Z\gamma$, $W\gamma$, $Z\gamma\gamma$, $W\gamma\gamma$ samples for e's, μ's, τ's ([2, 5, 6])
- $e \to \gamma$ (See Ref. [2], Section 3.2)
  - use events with back-to-back $e\gamma$ with $M_{e\gamma}$ within 10 GeV of M_{Z^0}
- $jet \to \gamma$ (Section 3.1)
  - use the calorimeter isolation for photons (similar to the Run I method). When the statistics is low and for the cross-checks, scale the number from 305 pb^{-1}.
- Jets faking ℓ and $\not\!\!E_T$ (Section 3.3)
  - use the track isolation method (same as documented in cdf7550)
- $t\bar{t}\gamma$ MC [7]
  - MadGraph sample. Expect small contribution, will contribute to a high-H_T region.
- kaons decays-in-flight (Section 3.4)
  - will use the number of transitions in DIF and $Z^0 \to \mu^+\mu^-$ samples

3.1 $jet \to \gamma$

High P_T photons are copiously created from hadron decays in jets initiated by a scattered quark or gluon. In particular, mesons such as the π^0 or η decay to photons which may satisfy the photon selection criteria. The numbers of lepton-plus-misidentified-jet events expected in the $\ell\gamma\not\!\!E_T$ and $\ell\ell\gamma$ samples are determined by measuring energy in the calorimeter nearby the photon candidate.

For each of the four samples, $e\gamma\not\!\!E_T$, $\mu\gamma\not\!\!E_T$, $ee\gamma$, and $\mu\mu\gamma$, Figure 2 shows the distribution in the total (electromagnetic plus hadronic) calorimeter energy, E_T^{Iso}, in a cone in η-ϕ space around the photon candidate. This distribution is then fitted to the shape measured for electrons from $Z^0 \to e^+e^-$ decay plus a linear background.

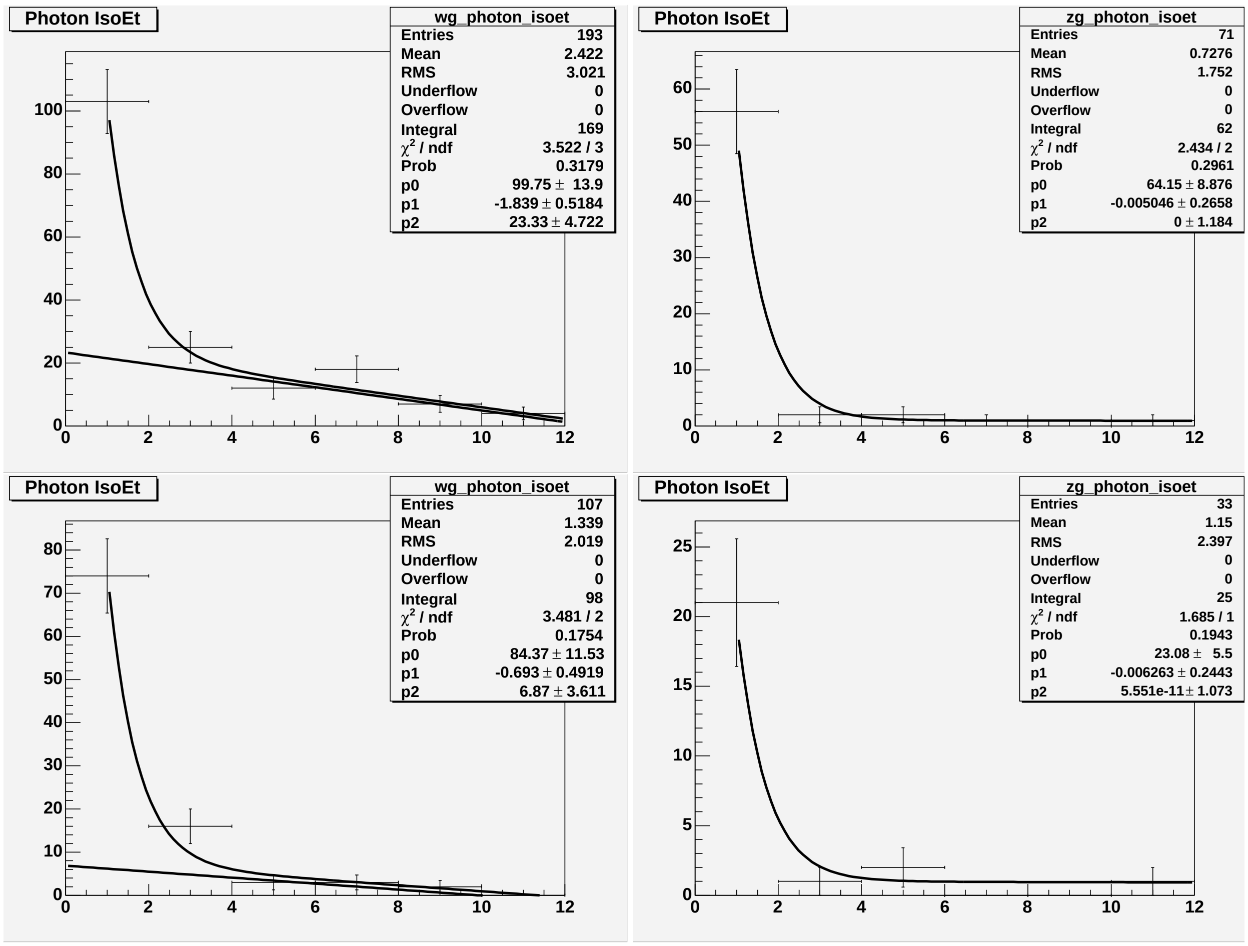

Figure 2: The method and data used to estimate the number of background events from jets misidentified as photons. For each of the four samples, $e\gamma\not\!\!E_T$ (left top), $\mu\gamma\not\!\!E_T$ (right top), $ee\gamma$ (left bottom), and $\mu\mu\gamma$ (right bottom), the number of events is plotted versus the total (electromagnetic plus hadronic) calorimeter energy, E_T^{Iso}, in a cone in η-ϕ space around the photon. This distribution is then fitted to the shape measured for electrons from $Z^0 \to e^+e^-$ decay plus a linear background.

To verify the linear behaviour of the background we create fake photon sample. To create the sample we require $\chi^2_{CES} > 20$ to reject real photons; we also ommit calorimeter and track isolation requirements. The distribution in the total calorimeter energy, E_T^{Iso}, in a cone in η-ϕ space around the fake photon candidate, is shown in Figure 3.

The predicted number of events with jets misidentified as photons is 27.7 ± 6.00 for the $\ell\gamma\not\!\!E_{\mathrm{T}}$ signature and 0.0 ± 1.60 for $\ell\ell\gamma$. We find that the backgrounds from jets misidentified as photons in the dilepton samples is very small.

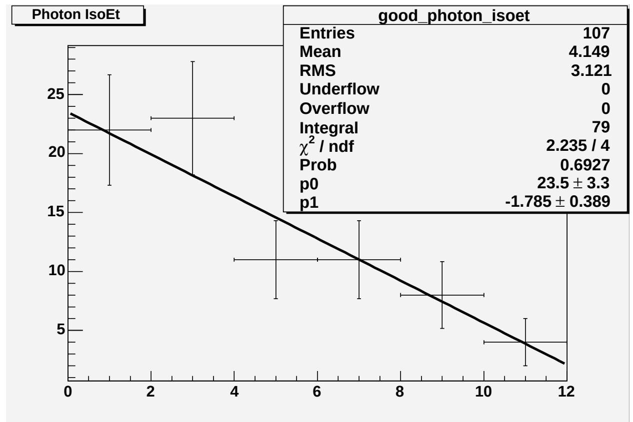

Figure 3: The distribution in the total calorimeter energy, $\mathrm{E}_{\mathrm{T}}^{Iso}$, in a cone in η-ϕ space around the fake photon candidate. This distribution is then fitted with a linear function.

The numbers of lepton-plus-misidentified-jet events expected in the $\ell\gamma\gamma$ and $e\mu\gamma$ samples are determined by measuring the jet E_{T} spectrum in $\ell\gamma$+jet, ℓ+jets and $e\mu$+jet samples, respectively, and then multiplying by the probability of a jet being misidentified as a photon, $P_{\gamma}^{jet}(\mathrm{E}_{\mathrm{T}})$, which is measured in data samples triggered on jets. The uncertainty on the number of such events is calculated by using the measured jet spectrum and the upper and lower bounds on the E_{T}-dependent misidentification rate.

The misidentification rate is $P_{\gamma}^{jet} = (6.5 \pm 3.3) \times 10^{-4}$ for $\mathrm{E}_{\mathrm{T}}^{\gamma} = 25\ GeV$, and $(4.0 \pm 4.0) \times 10^{-4}$ for $\mathrm{E}_{\mathrm{T}}^{\gamma} = 50\ GeV$ [8]. The predicted number of events with jets misidentified as photons is 0.09 ± 0.090 for the $\ell\gamma\gamma$ signature and 0.05 ± 0.00700 for $e\mu\gamma$.

3.2 $e \rightarrow \gamma$

The probability that an electron undergoes hard bremsstrahlung and is misidentified as a photon, P_{γ}^{e}, is measured from the photon control sample. The number of misidentified $e\gamma$ events divided by twice the number of ee events gives P_{γ}^{e}=(1.6 ± 0.2)%. Applying this misidentification rate to electrons in the inclusive lepton samples, we find 9.59 ± 0.76 and 0.38 ± 0.11 events pass the selection criteria for the $\ell\gamma\not\!\!E_{\mathrm{T}}$ and $\ell\ell\gamma$ searches, respectively. For the $\ell\gamma\gamma$ search we estimate this background to be 0.413 ± 0.12.

3.3 Jets faking ℓ and $\not\!\!E_{\mathrm{T}}$

We have estimated the background due to events with jets misidentified as $\ell\gamma\not\!\!E_{\mathrm{T}}$ or $\ell\ell\gamma$ signatures by studying the total P_{T} of tracks in a cone in $\eta - \varphi$ space of radius $R = 0.4$ around the lepton track. We estimate there are 15.0 ± 4.12 and 0.0 ± 0.20 events in the $\ell\gamma\not\!\!E_{\mathrm{T}}$ and $\ell\ell\gamma$ signatures, respectively.

We use the same method to estimate QCD (Jets faking ℓ and $\not\!\!E_{\mathrm{T}}$)background as for first 305 pb^{-1} [2].

We define four samples samples:

- Non-W/Z sample: 1 ℓ + jet(s), no W or Z candidates

Track Iso Region, GeV	$e\gamma \not\!\!E_T$	$ee\gamma$	$\mu\gamma \not\!\!E_T$	$\mu\mu\gamma$
2.0, 4.0	16±0.44	0±0.21	0±0.13	0±0.088
2.5, 4.5	14±0.42	0±0.2	0±0.13	0±0.085
2.5, 5.0	16±0.47	0±0.2	0±0.11	0±0.076
3.0, 4.5	14±0.42	0±0.2	0±0.13	0±0.085
3.0, 5.0	16±0.47	0±0.2	0±0.11	0±0.076
Average	$15.0 \pm 4.0(stat)$ $\pm 1.0(sys)$	$0.0 \pm 0.1(stat)$ $\pm 0(sys)$	$0.0 \pm 0.2(stat)$ $\pm 0(sys)$	$0.0 \pm 0.1(stat)$ $\pm 0(sys)$

Table 1: QCD (Jet faking lepton and $\not\!\!E_T$) background estimates. To estimate systematics we vary track iso regions. Note that statistical errors on data numbers are not included in this table in this revision of the note.

- Signal Sample: $\ell\gamma \not\!\!E_T$ or $ll\gamma$
- Golden-Lepton: Tight e's, CC $Z^0 \to e^+e^-$, Tight μ's $Z^0 \to \mu^+\mu^-$, close to Z mass
- Jet Faking Photon: $\ell j \not\!\!E_T$ or $\ell\ell j$

We define three track isolation regions:

- Track-Isolated: 0< Track Iso < 2
- Non-Track-Isolated: Track Iso >4
- 2< Track Iso <4

We estimate the background as follows:

- Estimate fraction of *golden* leptons with bad Track Iso
- Estimate fraction of *non-W/Z* leptons with good Track Iso
- Estimate *QCD(Jet faking lepton and $\not\!\!E_T$)* background
- Vary Track Iso Regions to get systematics (Table 1)

3.4 Misreconstructed muons ("Decays in Flight")

A muon background that escapes the above method is when a low-momentum hadron, not in an energetic jet, decays to a muon in a configuration that a high-momentum track is reconstructed from the initial track segment due to the hadron and the secondary track segment from the muon [1] The contribution from this background is estimated by identifying tracks consistent with a "kink" in the COT. We count the number of times that, proceding radially along a COT track, a 'hit' on the n+1 layer is on the other side of the fitted track from the hit on the nth layer. Real tracks will have hits distributed on both sides of the fit, and will therefore have many 'transitions'. A mis-measured track from a 5-GeV K^+, on the other hand, will consist of two intersecting low-momentum arcs fit by a high momentum track, and will have a small number of transitions.

Figure 4 shows the number of transitions in muons in the $Z^0 \to \mu^+\mu^-$ control sample, and in a sample enriched in hadron decays by selecting muons that have large impact parameters. We estimate there are 2.3 ± 0.72 and 0.0 ± 0.20 events from decay-in-flight in the $\mu\gamma \not\!\!E_T$ and $\mu\mu\gamma$ samples, respectively.

To estimate the background from the misreconstructed muons ("Decays in Flight", DIF), we define four samples samples:

[1] Decays before or after the COT volume result in a correct measurement of the momentum and are included in the other background estimate.

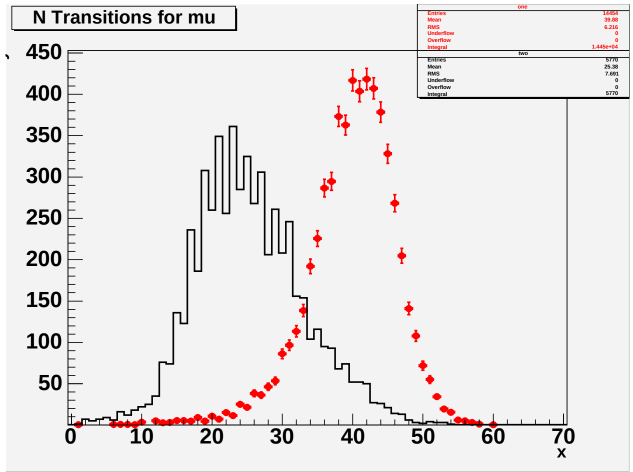

Figure 4: The method and data used to estimate the number of background muons from low-momentum hadrons decaying in flight. The number of transitions in muons in the $Z^0 \to \mu^+\mu^-$ sample is shown as red points. The number of transitions in muons in the sample enriched in hadron decays is shown as a black histogram.

- $W^{bad\ d_0}$: μ with track d_0 >0.2 cm, $\not\!\!E_T > 25$, $N_{jets} > 0$
- Signal Sample: $\ell\gamma\not\!\!E_T$ or $ll\gamma$
- Golden-Lepton: Tight μ's $Z^0 \to \mu^+\mu^-$, within 10 GeV of Z mass, back-to-back
- Jet Faking Photon: $\ell j \not\!\!E_T$ or $\ell\ell j$

We define three N_{tr} regions:

- Good: N_{tr} >40
- Bad: N_{tr} <30
- Intermediate: 30< N_{tr} <40

We estimate the DIF background as follows:

- Estimate fraction of *golden* muons in bad region
- Estimate fraction of $W^{bad\ d_0}$ muons in good region
- Estimate **DIF** background
- Vary N_{tr} Regions to get systematics (Table 2)

N_{tr} regions	$\mu\gamma\not\!\!E_T$	$\mu\mu\gamma$
40, 45	1.9±0.68	0±0.16
35, 40	2.7±0.59	0±0.13
30, 40	2.1±0.62	0±0.14
35, 45	2.7±0.58	0±0.13
30, 35	2.1±0.62	0±0.14
Average	$2.3 \pm 0.6(stat) \pm 0.4(sys)$	$0.0 \pm 0.2(stat) \pm 0.0(sys)$

Table 2: Decay-in-flight background estimates. To estimate systematics we vary N_{tr} regions.

4 Search for $\ell\gamma + X$: Results

4.1 The Inclusive $\ell\gamma + X$ Event Sample

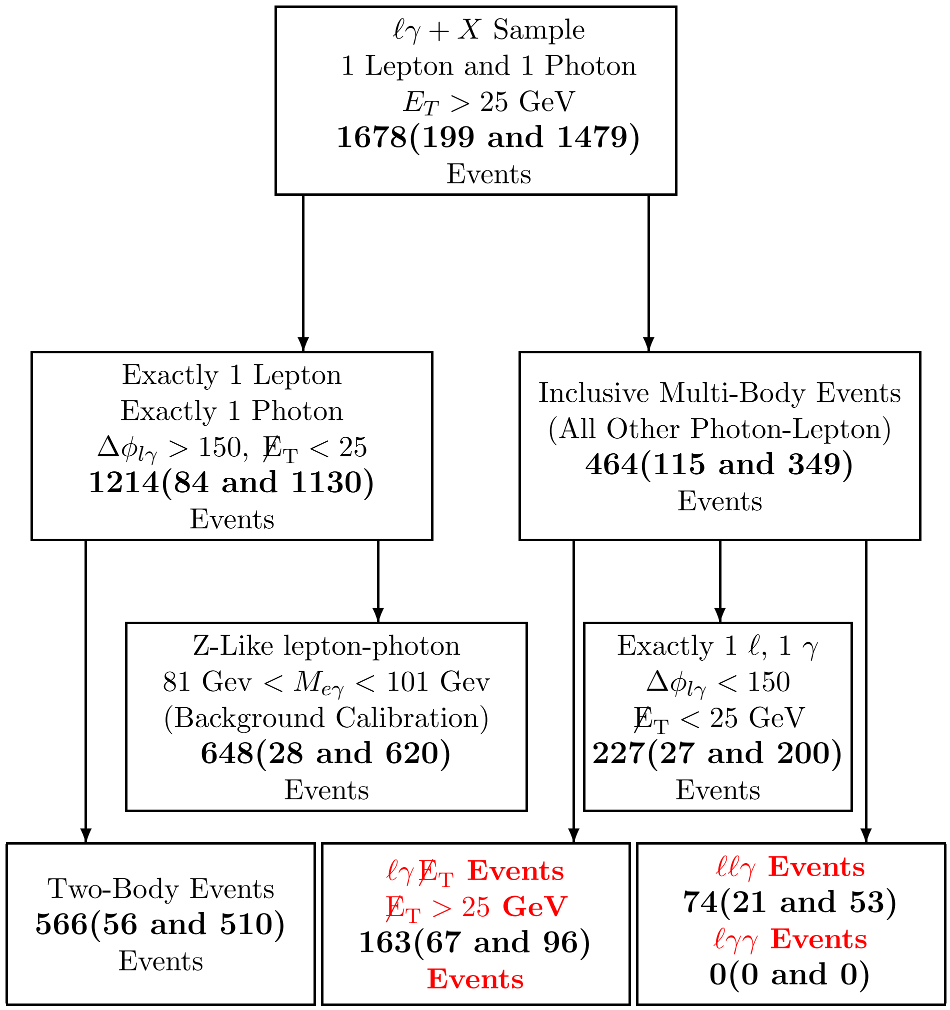

Figure 5: $\ell\gamma + X$ Sample: the Subsets of Inclusive $\ell\gamma$ Events Analyzed. The number of events in each subcategory is given as a sum of muons and electrons

A total of 1678 events, 1479 inclusive $e\gamma$ and 199 inclusive $\mu\gamma$ candidates, pass the $\ell\gamma$ selection criteria. Of the 1479 inclusive $e\gamma$ events, 1130 have the electron and photon within 30° of back-to-back in φ, $\not\!\!E_{\rm T} < 25\ GeV$, and no additional leptons or photons. These are dominated by $Z^0 \to e^+e^-$ decays in which one of the electrons radiates a high-$E_{\rm T}$ photon while traversing the material inside the COT active volume, leading to the observation of an electron and a photon approximately back-to-back in φ, with an $e\gamma$ invariant mass close to the Z^0 mass.

4.2 $\ell\gamma\not\!\!E_{\rm T}$

The first search we perform is in the $\ell\gamma\not\!\!E_{\rm T}+X$ subsample, defined by requiring that an event contain $\not\!\!E_{\rm T} > 25\ GeV$ in addition to the γ and "tight" lepton. Of the 1678 $\ell\gamma$ events, 96 $e\gamma\not\!\!E_{\rm T}$ events and 67 $\mu\gamma\not\!\!E_{\rm T}$ events pass the $\not\!\!E_{\rm T}$ requirement. Figures 6 and 7 show the observed distributions in a)

Table 3: A comparison of the numbers of events predicted by the SM and the observations for the $\ell\gamma\not\!\!E_T$ search. The SM predictions are dominated by $W\gamma$ and $Z\gamma$ production [9, 10, 11]. Other contributions come from $W\gamma\gamma$ and $Z\gamma\gamma$, leptonic τ decays, and misidentified leptons, photons, or $\not\!\!E_T$.

CDF Run II Preliminary, $929pb^{-1}$			
Lepton+ Gamma + $\not\!\!E_T$ Events			
Standard Model Source	$e\gamma\not\!\!E_T$	$\mu\gamma\not\!\!E_T$	$(e+\mu)\gamma\not\!\!E_T$
$W^{\pm}\gamma$	41.65 ± 4.84	29.85 ± 5.62	71.50 ± 10.01
$Z^0/\gamma + \gamma$	3.65 ± 1.31	14.10 ± 2.36	17.75 ± 3.65
$W^{\pm}\gamma\gamma$	0.32 ± 0.042	0.18 ± 0.025	0.50 ± 0.064
$Z^0/\gamma + \gamma\gamma$	0.087 ± 0.012	0.38 ± 0.048	0.47 ± 0.058
$t\bar{t}\gamma$	0.22 ± 0.029	0.13 ± 0.019	0.35 ± 0.045
$Z^0 \rightarrow e^+e^-, e \rightarrow \gamma$	9.59 ± 0.76	–	9.59 ± 0.76
Jet faking γ	21.5 ± 4.80	6.2 ± 3.60	27.7 ± 6.00
$\tau\gamma$ contribution	2.15 ± 0.56	0.76 ± 0.24	2.91 ± 0.65
QCD(Jets faking ℓ and $\not\!\!E_T$)	15.0 ± 4.12	0.0 ± 0.100	15.0 ± 4.12
DIF (Decays-In-Flight)	–	2.3 ± 0.72	2.3 ± 0.72
Total	$94.17 \pm 4.71(stat)$ $\pm 6.64(sys)$	$53.90 \pm 1.94(stat)$ $\pm 6.84(sys)$	$148.07 \pm 5.10(stat)$ $\pm 11.93(sys)$
	$94.17 \pm 8.14(tot)$	$53.90 \pm 7.11(tot)$	$148.07 \pm 12.97(tot)$
Observed in Data	96	67	163

the E_T of the photon; b) the E_T of the lepton; c) $\not\!\!E_T$; and d) the transverse mass of the $\ell\gamma\not\!\!E_T$ system, where $M_T = [(E_T^{\ell} + E_T^{\gamma} + \not\!\!E_T)^2$ - $(\vec{E}_T^{\ell} + \vec{E}_T^{\gamma} + \vec{\not\!\!E}_T)^2]^{1/2}$.

The distributions for the electrons and for the muons are combined on the Figure 8.

The predicted and observed totals for the $\ell\gamma\not\!\!E_T$ search are shown in Table 9.

Figure 9 shows the distributions for the $e\gamma\not\!\!E_T$ sample in a) H_T, the sum of the transverse energies of the electron, photon, jets and $\not\!\!E_T$; b) the distance in η-ϕ space between the photon and electron; c) the angular separation in ϕ between the electron and the missing transverse energy, $\not\!\!E_T$; and d) the transverse mass of the $\ell\gamma\not\!\!E_T$ system. The histograms show the expected SM contributions, including estimated backgrounds from misidentified photons and leptons.

Figure 10 shows the same distributions for the $\mu\gamma\not\!\!E_T$ sample. The distributions for the electrons and for the muons are combined on the Figure 11.

4.3 $\ell\ell\gamma$

A second search, for the $\ell\ell\gamma + X$ signature, is constructed by requiring another e or μ in addition to the "tight" lepton and the γ.

The predicted and observed totals for the $\ell\ell\gamma$ search are shown in Table 10.

The $\ell\ell\gamma$ search criteria select 74 events (53 $ee\gamma$ and 21 $\mu\mu\gamma$) of the 1678 $\ell\gamma$ events. No $e\mu\gamma$ events are observed. Figure 12 shows the observed distributions in a) the E_T of the photon; b) the E_T of the electrons; c) the 2-body mass of the dilepton system; and d) the 3-body mass $m_{ee\gamma}$.

The corresponding distributions for the $\mu\mu\gamma$ sample are shown in Figure 13. The distributions for the electrons and for the muons are combined on the Figure 14.

Figure 15 shows the distributions for the $ee\gamma$ sample in a) H_T, the sum of the transverse

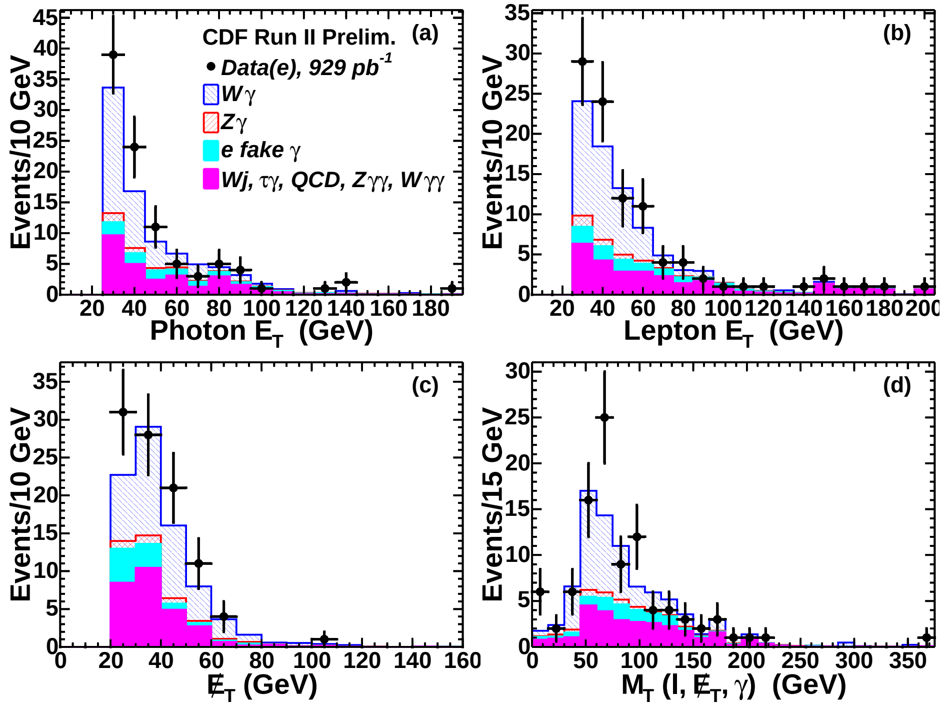

Figure 6: The distributions for events in the $e\gamma\not{E}_{\mathrm{T}}$ sample (points) in a) the $\mathrm{E_T}$ of the photon; b) the $\mathrm{E_T}$ of the electron; c) the missing transverse energy, $\not{E}_{\mathrm{T}}$; and d) the transverse mass of the $e\gamma\not{E}_{\mathrm{T}}$ system. The histograms show the expected SM contributions, including estimated backgrounds from misidentified photons and electrons.

Table 4: A comparison of the numbers of events predicted by the SM and the observations for the $\ell\gamma\not{E}_{\mathrm{T}}$ search. The SM predictions are dominated by $Z\gamma$ production [9, 10, 11]. Other contributions come from $Z\gamma\gamma$, and misidentified leptons, photons, or $\not{E}_{\mathrm{T}}$.

CDF Run II Preliminary, $929pb^{-1}$			
Multi-Photon + Lepton Predicted Events			
SM Source	$e\gamma\gamma$	$\mu\gamma\gamma$	$\ell\gamma\gamma$
$Z^0\gamma$	37.85 ± 4.65	25.55 ± 2.88	63.40 ± 7.48
$Z^0\gamma\gamma$	0.72 ± 0.088	0.40 ± 0.050	1.12 ± 0.13
Z^0+Jet, jet faking γ	0.0 ± 1.20	0.0 ± 1.10	0.0 ± 1.60
$Z^0 \rightarrow e^+e^-, e \rightarrow \gamma$	0.38 ± 0.11	–	0.38 ± 0.11
QCD (Non-WZ) fakes	0.0 ± 0.20	0.0 ± 0.100	0.0 ± 0.20
DIF (Decays-In-Flight)	–	0.0 ± 0.20	0.0 ± 0.20
Total	$38.95 \pm 0.71(stat)$ $\pm 4.75(sys)$	$25.95 \pm 0.56(stat)$ $\pm 3.04(sys)$	$64.93 \pm 0.89(stat)$ $\pm 7.60(sys)$
	$38.95 \pm 4.80(tot)$	$25.95 \pm 3.09(tot)$	$64.93 \pm 7.65(tot)$
Observed	53	21	74

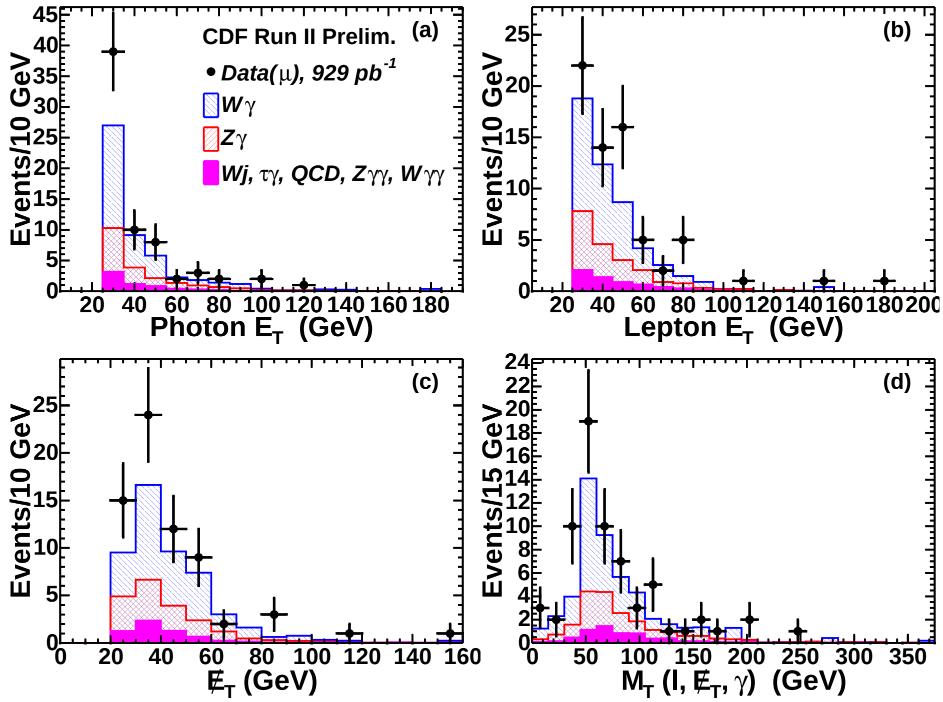

Figure 7: The distributions for events in the $\mu\gamma\not\!\!E_{\rm T}$ sample (points) in a) the $\rm E_T$ of the photon; b) the $\rm E_T$ of the muon; c) the missing transverse energy, $\not\!\!E_{\rm T}$; and d) the transverse mass of the $\mu\gamma\not\!\!E_{\rm T}$ system. The histograms show the expected SM contributions, including estimated backgrounds from misidentified photons and muons.

energies of the electron, photon, jets and $\not\!\!E_{\rm T}$; b) the distance in η-ϕ space between the photon and each of the two electrons The histograms show the expected SM contributions, including estimated backgrounds from misidentified photons and electrons.

Figure 16 shows the same distributions for the $\mu\gamma\not\!\!E_{\rm T}$ sample.

The distributions for the electrons and for the muons are combined on the Figure 17.

We do not expect SM events with large $\not\!\!E_{\rm T}$ in the $\ell\ell\gamma$ sample; the Run I $ee\gamma\gamma\not\!\!E_{\rm T}$ event was of special interest in the context of supersymmetry [12] due to the large value of $\not\!\!E_{\rm T}$ $(55 \pm 7\ GeV)$. Figure 18 shows the distributions in $\not\!\!E_{\rm T}$ for the $\mu\mu\gamma$ and $ee\gamma$ subsamples of the $\ell\ell\gamma$ sample.

4.4 $e\mu\gamma$

The predicted and observed totals for the $e\mu\gamma$ search are shown in Table 5. We observe no $e\mu\gamma$ events, versus the expectation of 1.01 ± 0.33 events.

4.5 $\ell\gamma\gamma$

The predicted and observed totals for the $\ell\gamma\gamma$ search are shown in Table 6. We observe no $\ell\gamma\gamma$, versus the expectation of 0.62 ± 0.15 events.

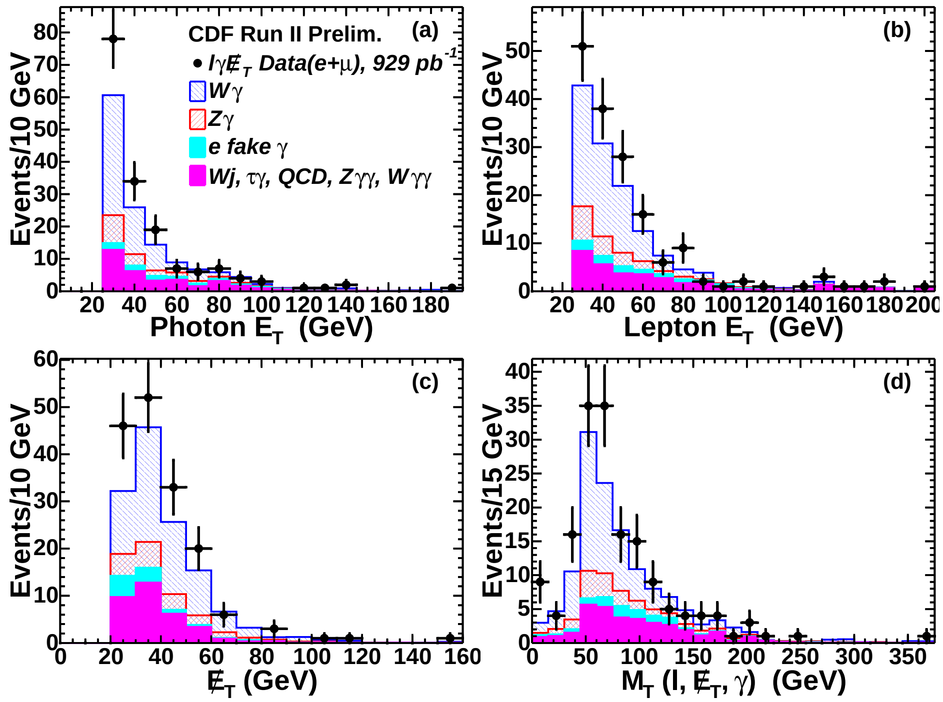

Figure 8: The distributions for events in the $\ell\gamma \not\!\!E_T$ sample (points) in a) the $\mathrm{E_T}$ of the photon; b) the $\mathrm{E_T}$ of the lepton (e or μ); c) the missing transverse energy, $\not\!\!E_T$; and d) the transverse mass of the $\ell\gamma \not\!\!E_T$ system. The histograms show the expected SM contributions, including estimated backgrounds from misidentified photons and leptons.

5 Acknowledgments

We thank Andrei Rostovtsev for his encouragement and support. We also owe thanks to Eduard Boos and Lev Dudko for their support and development of CompHep, and Tim Steltzer, Steve

Table 5: A comparison of the numbers of events predicted by the SM and the observations for the $e\mu\gamma$ search. The SM predictions are dominated by $Z\gamma$ production [9, 10, 11]. Other contributions come from $W\gamma$, $Z\gamma\gamma$, $W\gamma\gamma$, and misidentified leptons, photons, or $\not\!\!E_T$.

CDF Run II Preliminary, $929 pb^{-1}$	
$e\mu$ + Photon + X Predicted Events	
Standard Model Source	$e\mu\gamma + X$
$Z^0\gamma$	0.66 ± 0.088
$W\gamma$	0.095 ± 0.18
$Z^0\gamma\gamma$	0.057 ± 0.0054
$W\gamma\gamma$	0.011 ± 0.0028
$e\mu j,\ j \to \gamma$	0.05 ± 0.00700
$ee\mu,\ e \to \gamma$	0.063 ± 0.045
$\tau\gamma$ contribution	0.089 ± 0.18
Total	1.01 ± 0.33
Observed	0

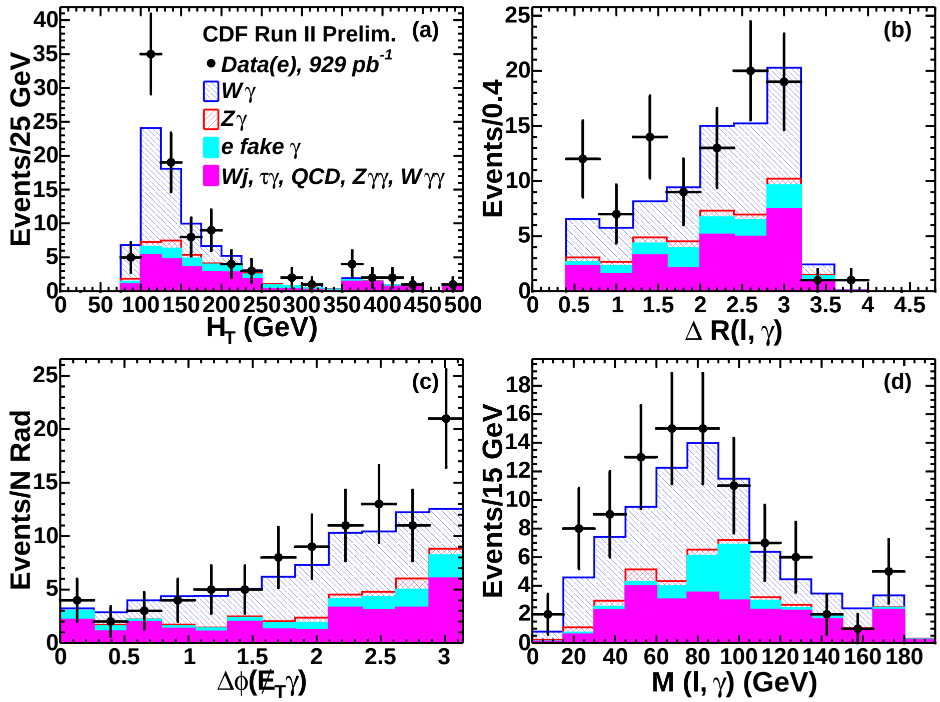

Figure 9: The distributions for events in the $e\gamma\not{E}_T$ sample (points) in a) H_T, the sum of the transverse energies of the electron, photon, jets and $\not{E}_T$; b) the distance in η-ϕ space between the photon and electron; c) the angular separation in ϕ between the electron and the missing transverse energy, $\not{E}_T$; and d) the transverse mass of the $e\gamma\not{E}_T$ system. The histograms show the expected SM contributions, including estimated backgrounds from misidentified photons and electrons.

Mrenna, and Fabio Maltoni for their similar responsiveness for MadGraph and Pythia. Alexander Belyaev, and Alexander Sherstnev generated the CompHep $W\gamma\gamma$ and $Z\gamma\gamma$ datasets, respectively, for us. Uli Baur provided wisdom on the effective Born approximation parameters for the LO parameters. Steve Levy, Carla Pilcher, Alexander Paramonov, and Collin Wolfe provided invaluable

Table 6: A comparison of the numbers of events predicted by the SM and the observations for the $\ell\gamma\gamma$ search. The SM predictions are dominated by $Z\gamma\gamma$ production [9, 11]. Dominant contribution comes from misidentified photons.

CDF Run II Preliminary, $929 pb^{-1}$			
Multi-Photon + Lepton Predicted Events			
SM Source	$e\gamma\gamma$	$\mu\gamma\gamma$	$\ell\gamma\gamma$
$W^{\pm}\gamma\gamma$	0.021 ± 0.0043	0.015 ± 0.0034	0.036 ± 0.0055
$Z^0\gamma\gamma$	0.045 ± 0.0051	0.038 ± 0.0045	0.083 ± 0.0068
$Z^0\gamma$, $e \to \gamma$	0.413 ± 0.116	-	0.413 ± 0.116
ℓjj, $\ell\gamma j$, $j \to \gamma$	0.04917 ± 0.049	0.05060 ± 0.051	0.09 ± 0.090
Total	0.53 ± 0.13	0.10 ± 0.051	0.62 ± 0.15
Observed	0	0	0

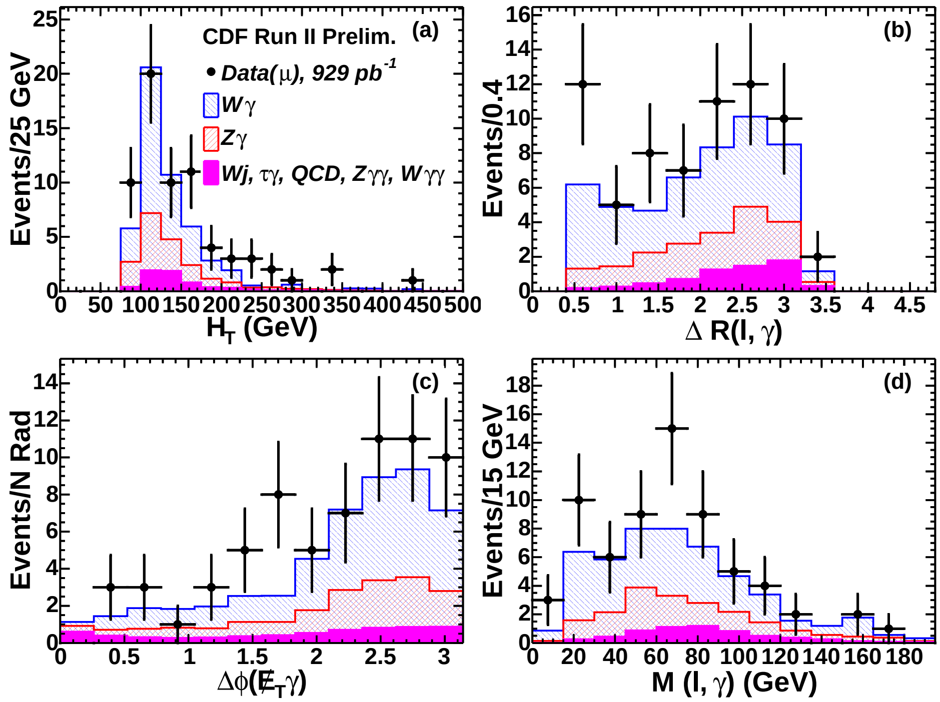

Figure 10: The distributions for events in the $\mu\gamma\not\!\!E_T$ sample (points) in a) $\mathrm{H_T}$, the sum of the transverse energies of the muon, photon, jets and $\not\!\!E_T$; b) the distance in η-ϕ space between the photon and muon; c) the angular separation in ϕ between the muon and the missing transverse energy, $\not\!\!E_T$; and d) the transverse mass of the $\mu\gamma\not\!\!E_T$ system. The histograms show the expected SM contributions, including estimated backgrounds from misidentified photons and muons.

support for the UCntuple and datasets. We also would like to thank our CDF collaborators Kathy Copic, Ray Culbertson, Max Goncharov, Helen Hayward, Beate Heinemann, Heather Gerberich, Al Goshaw, Mike Kirby, Jane Nachtman, Alexei Safonov, Tara Shears, Reda Tafirout, Stan Thompson, Jason Tsui, Soushi Tsuno, Song Ming Wang, and Un-Ki Yang for their many contributions.

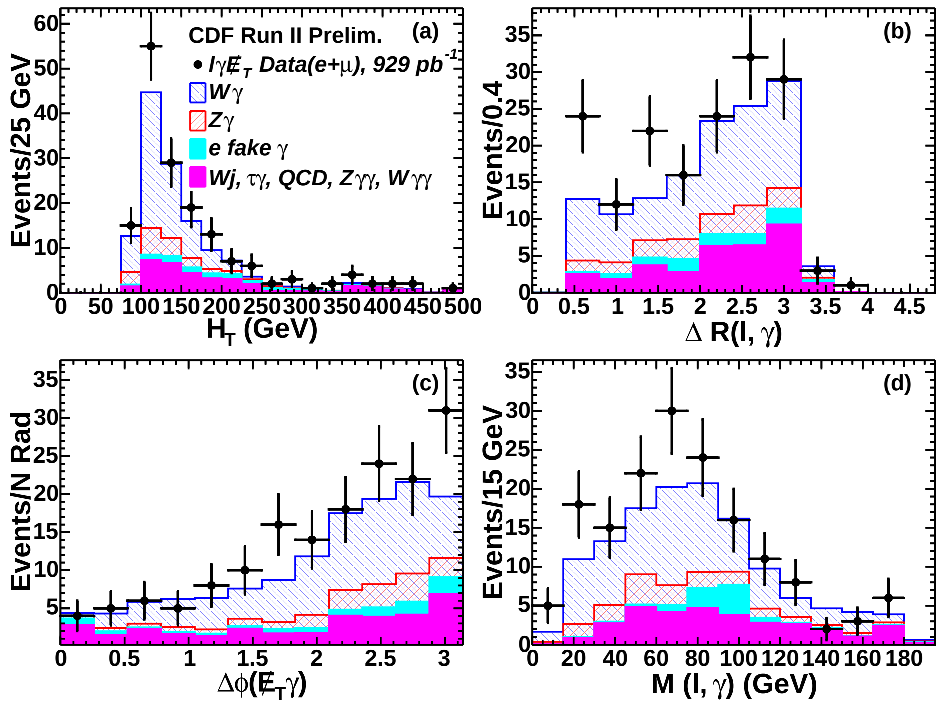

Figure 11: The distributions for events in the $\ell\gamma\not{E}_T$ sample (points) in a) H_T, the sum of the transverse energies of the muon, photon, jets and $\not{E}_T$; b) the distance in η-ϕ space between the photon and muon; c) the angular separation in ϕ between the muon and the missing transverse energy, $\not{E}_T$; and d) the transverse mass of the $\mu\gamma\not{E}_T$ system. The histograms show the expected SM contributions, including estimated backgrounds from misidentified photons and leptons.

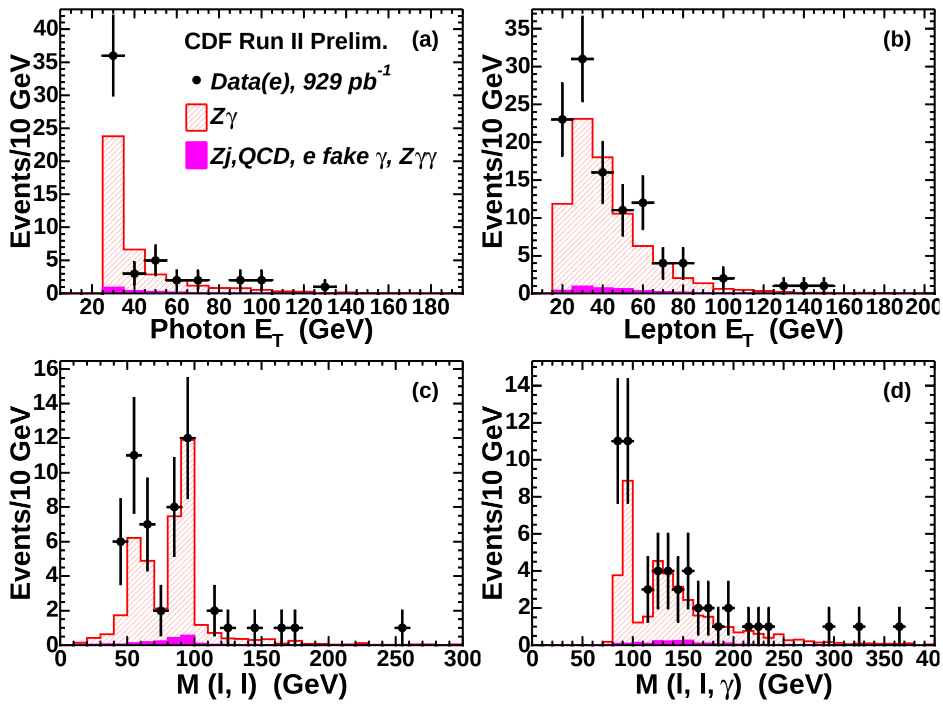

Figure 12: The distributions for events in the $ee\gamma$ sample (points) in a) the $\mathrm{E_T}$ of the photon; b) the $\mathrm{E_T}$ of the electrons (two entries per event); c) the 2-body mass of the dilepton system; and d) the 3-body mass $m_{\ell\ell\gamma}$. The histograms show the expected SM contributions.

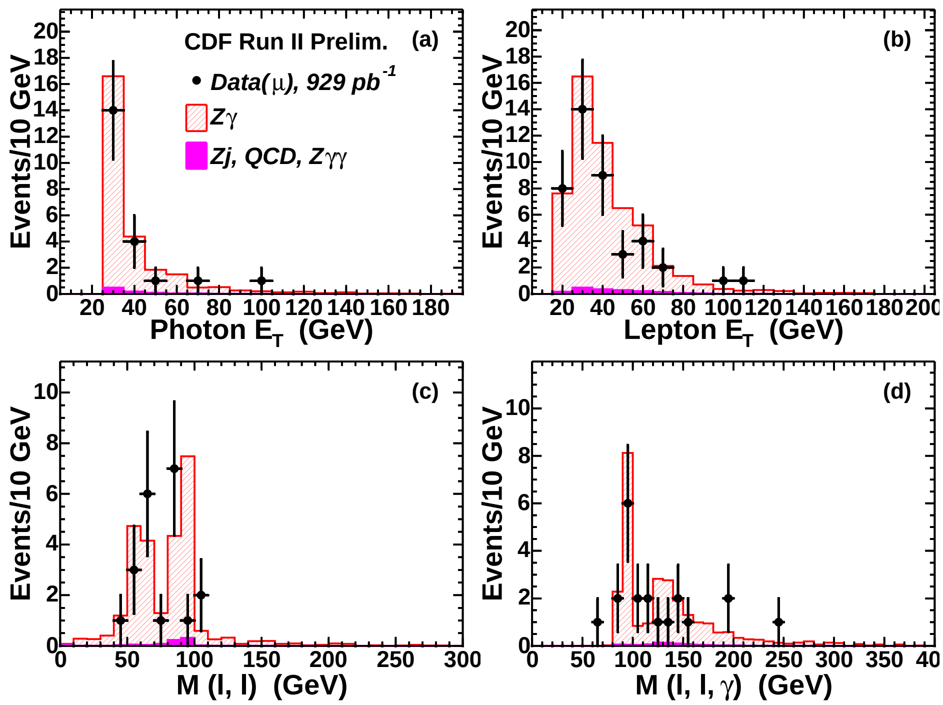

Figure 13: The distributions for events in the $\mu\mu\gamma$ sample (points) in a) the $\mathrm{E_T}$ of the photon; b) the $\mathrm{E_T}$ of the muons (two entries per event); c) the 2-body mass of the dilepton system; and d) the 3-body mass $m_{\mu\mu\gamma}$. The histograms show the expected SM contributions.

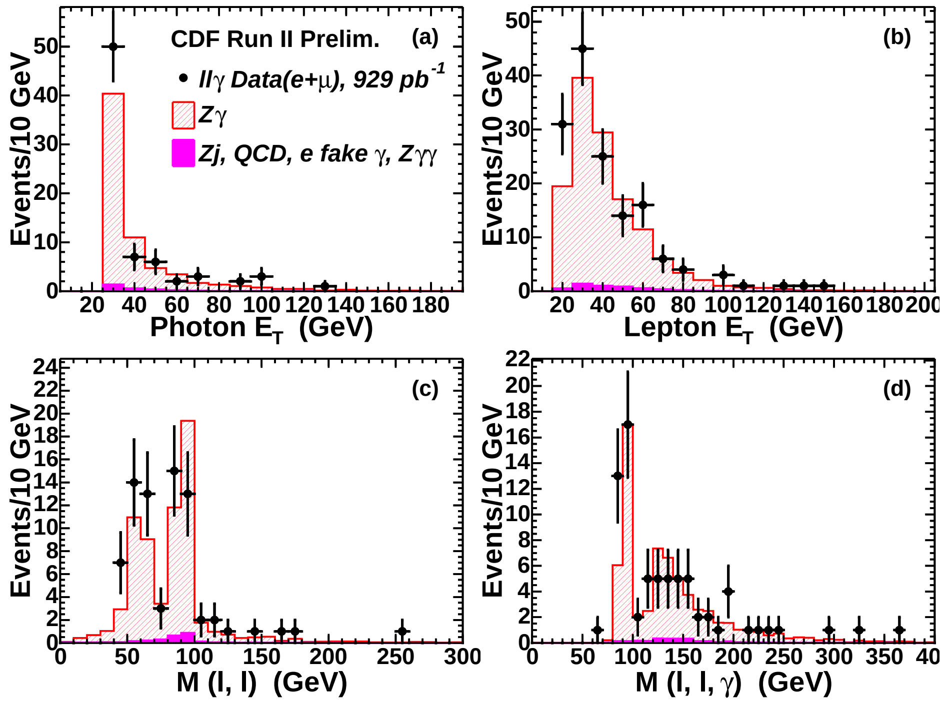

Figure 14: The distributions for events in the $\ell\ell\gamma$ sample (points) in a) the E_T of the photon; b) the E_T of the leptons (two entries per event); c) the 2-body mass of the dilepton system; and d) the 3-body mass $m_{\ell\ell\gamma}$. The histograms show the expected SM contributions.

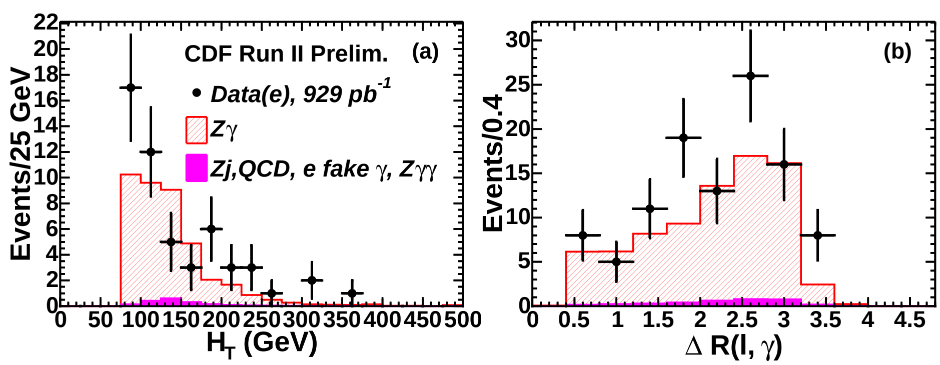

Figure 15: The distributions for events in the $ee\gamma$ sample (points) in a) H_T, the sum of the transverse energies of the electron, photon, jets and $\not\!\!E_T$; b) the distance in η-ϕ space between the photon and each of the two electrons. The histograms show the expected SM contributions, including estimated backgrounds from misidentified photons and electrons.

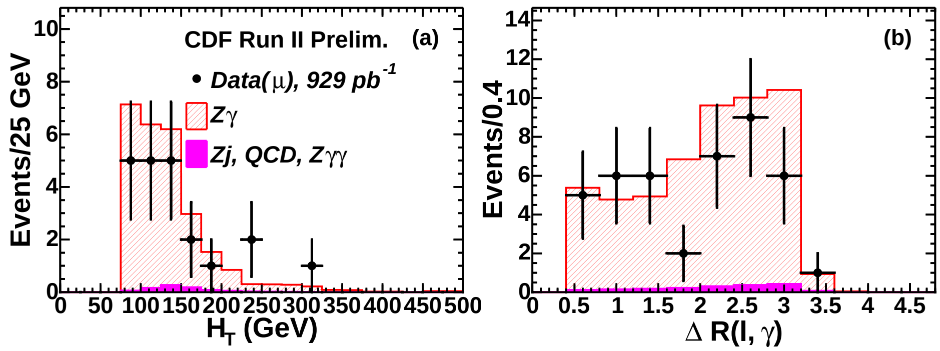

Figure 16: The distributions for events in the $\mu\mu\gamma$ sample (points) in a) $\mathrm{H_T}$, the sum of the transverse energies of the muon, photon, jets and $\not\!\!E_{\mathrm{T}}$; b) the distance in η-ϕ space between the photon and each of the two muons. The histograms show the expected SM contributions, including estimated backgrounds from misidentified photons and muons.

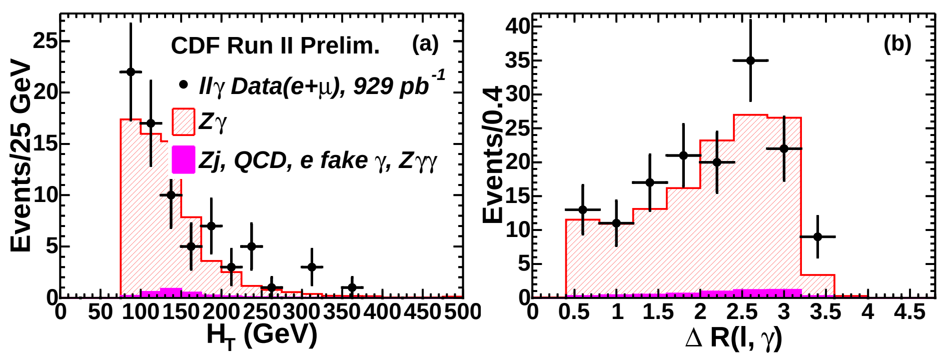

Figure 17: The distributions for events in the $\ell\ell\gamma$ sample (points) in a) $\mathrm{H_T}$, the sum of the transverse energies of the muon, photon, jets and $\not\!\!E_{\mathrm{T}}$; b) the distance in η-ϕ space between the photon and each of the two leptons. The histograms show the expected SM contributions, including estimated backgrounds from misidentified photons and muons.

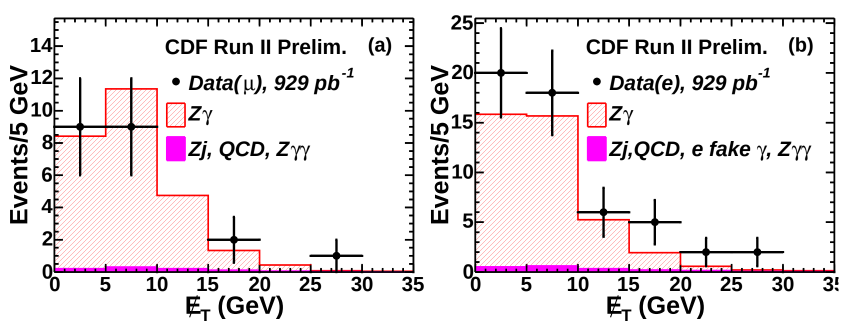

Figure 18: The distributions in missing transverse energy $\not\!\!E_{\mathrm{T}}$ observed in the inclusive search for a) $\mu\mu\gamma$ events and b) $ee\gamma$ events. The histograms show the expected SM contributions.

A Appendices

A.1 Checks of 5.x and 6.x jet corrections. Checks of two independent $\ell\gamma$ strips

I've done a check of two different lg strips. The code used (cdfsoft 611) is different from the one used for the publication (cdfsoft 533) based on 305 pb-1, and the main difference is the jet corrections (which changes a value of $\not\!\!E_{\mathrm{T}}$ in the events which contain jets). For the categories in which there is a difference between published numbers and the numbers obtained with 611 code we list values of $\not\!\!E_{\mathrm{T}}$ for 533 and 611 versions of the analysis code (which includes jet corrections).

Two independent strips:

strip/category	$\mu\gamma\not\!\!E_{\mathrm{T}}$	$e\gamma\not\!\!E_{\mathrm{T}}$	$\mu\mu\gamma$	$ee\gamma$
5.x, $\ell\gamma$(loginov)	17	25	12	19
6.x, $\ell\gamma$(shreyber)	17	28	12	19

Table 7: Two different strips, 6.x vs 5.x analysis code (including jet different jet corrections): number of observed events for different $\ell\gamma + X$ categories.

For three "additional" $e\gamma\not\!\!E_{\mathrm{T}}$ events:

	γ			ℓ					$\ell\gamma$		$\not\!\!E_{\mathrm{T}}$	
run/event	pt	phi	eta	type	pt	phi	eta	t	$\Delta\phi$	InvM	$\not\!\!E_{\mathrm{T}}$	phi
6.1.1 code, shreyber's strip												
161379/494836	97.30	-0.16	0.75	TCEM	148.8	2.11	0.19	1	2.27	228.9	26.84	-1.55
178744/1613754	65.78	0.21	-0.38	TCEM	75.45	-1.42	-0.78	1	1.63	107.0	26.40	2.48
186575/174332	25.38	2.26	-0.51	TCEM	42.24	0.95	0.68	1	1.32	57.5	25.71	-1.35
5.3.3 code, loginov's strip												
161379/494836	97.30	-0.16	0.75	TCEM	148.8	2.11	0.19	1	2.27	228.9	24.12	-1.58
178744/1613754	65.78	0.21	-0.38	TCEM	75.45	-1.42	-0.78	1	1.63	107.0	23.17	2.47
186575/174332	25.38	2.26	-0.51	TCEM	42.24	0.95	0.68	1	1.32	57.5	24.94	-1.33

Table 8: Two different strips, 6.x vs 5.x analysis code (including jet different jet corrections): three additional events from $e\gamma\not\!\!E_{\mathrm{T}}$ sample.

To conclude, both strips samples agree for 5.3.3 data, which adds confidence to the published numbers [1]. We will switch to latest jet corrections for 5.x and 6.x data [13].

A.2 Studies of the additional tracks in $\mu\gamma\not\!\!E_{\mathrm{T}}$ sample

We've compared 305 pb^{-1} of old data (0d datasets with good run list v7, cmx and silicon required, i.e. bits 1,1,1,1, no partial runs) to 610pb^{-1} of new data for $\mu\gamma$ events (0h and 0i datasets). We plot the distributions for $\mu\gamma\not\!\!E_{\mathrm{T}}$ (Figure 20) and $\mu\mu\gamma$(Figure 21) categories. We also compare the number of the additional tracks and distributions for the tracks for $\mu\gamma\not\!\!E_{\mathrm{T}}$ signature (Figure 22). We conclude that the number of the additional tracks scales with luminosity, and doesn't explain why we have more events than we predict in $\mu\gamma\not\!\!E_{\mathrm{T}}$ and less events than we predict in $\mu\mu\gamma$.

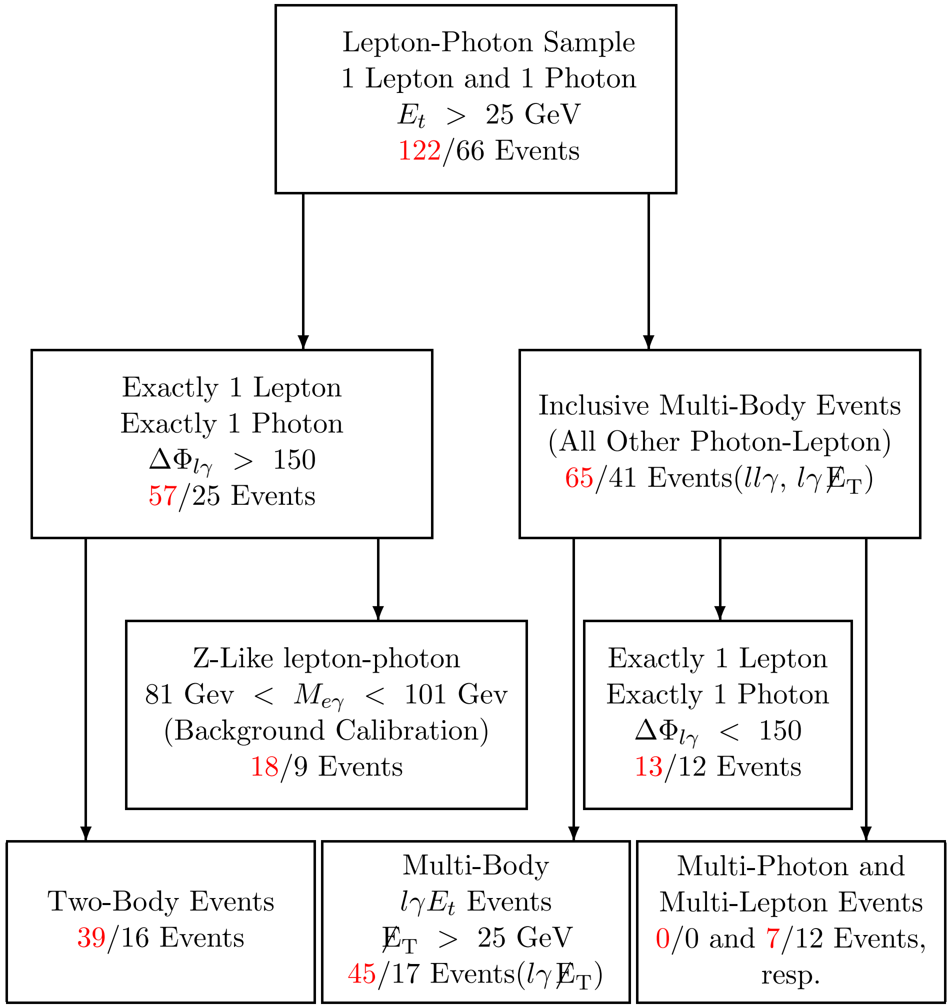

Figure 19: Photon-Muon Sample: the subsets of inclusive γl events to be analyzed. Numbers of events in the first 305 pb^{-1} is shown in black, number of events in new $610pb^{-1}$ is shown in red.

B Lepton-Photon Events: Observations (Back-Up. Plots contain error bars.)

B.1 The Number of Events Observed

Figure 23 shows the results of this classification for the inclusive electron data sample. We find 1479 electron-photon events, of which 349 are in the Inclusive Multi-Body category. Of these, 96 are classified as $\ell\gamma\not{E}_T$ events and 0 and 53 as Multi-Photon and Multi-Lepton events respectively.

Figure 24 shows the results for the inclusive muon sample.We find 199 muon-photon events, of which 115 are in the Inclusive Multi-Body category. Of these, 67 are classified as $\ell\gamma\not{E}_T$ events and 0 and 21 as Multi-Photon and Multi-Lepton events.

Figure 25 shows the sum of the electron and muon entries in the analysis subcategories. There are 163 $l\gamma\not{E}_T$ events(), 0 Multi-Photon events, and 74 Multi-Lepton events. It is these categories, shown in red in the figures, that are of particular interest due to the Run I results.

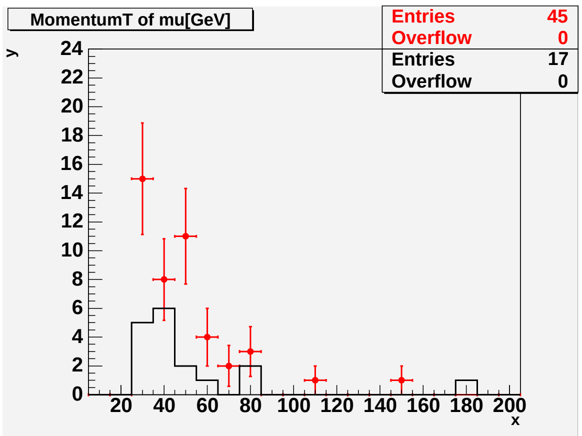

(a) Muon P_T

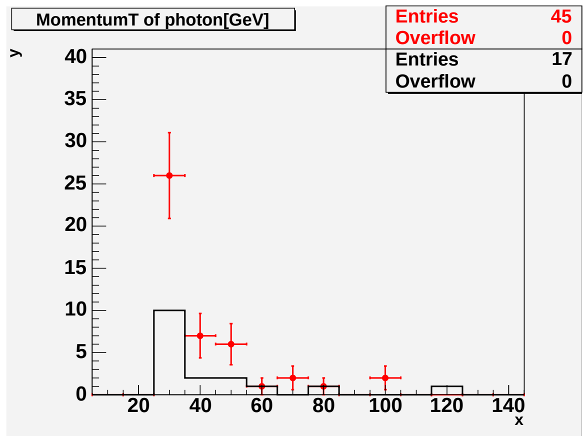

(b) Photon P_T

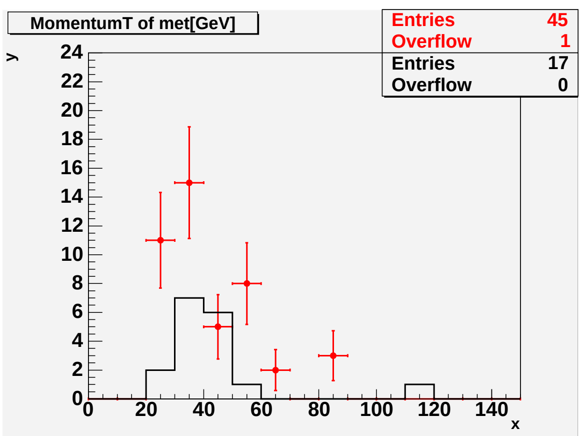

(c) $\not\!\!E_T$

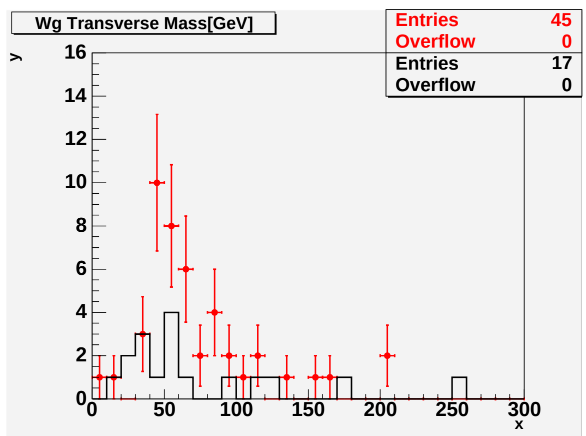

(d) $\ell\gamma\not\!\!E_T$ Invariant Mass

Figure 20: Lepton-Gamma-Met Distributions: Muon Channel. Numbers of events in the first 305 pb^{-1} is shown in black, number of events in new $610pb^{-1}$ is shown in red.

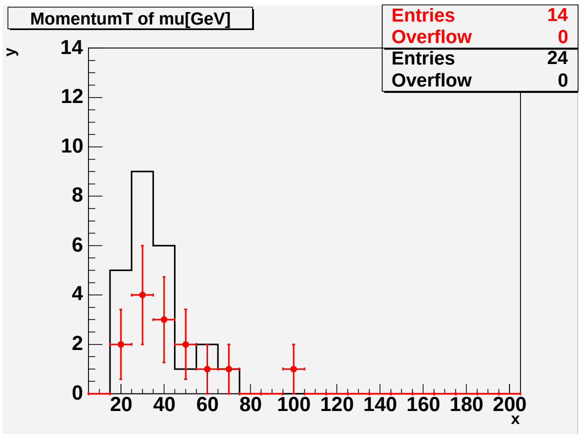

(a) Muon P_T

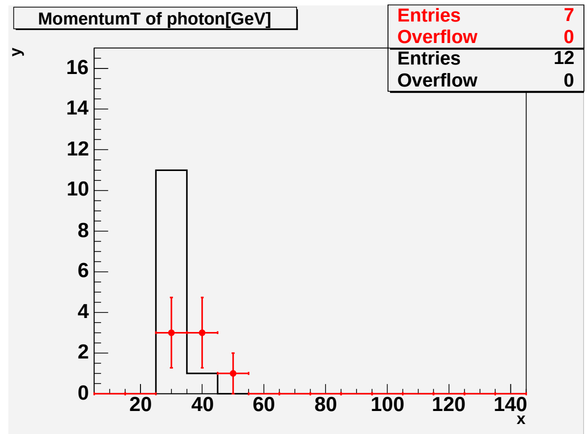

(b) Photon P_T

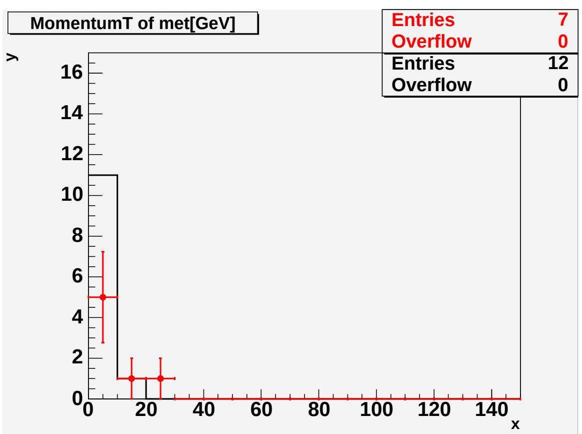

(c) $\not\!\!E_T$

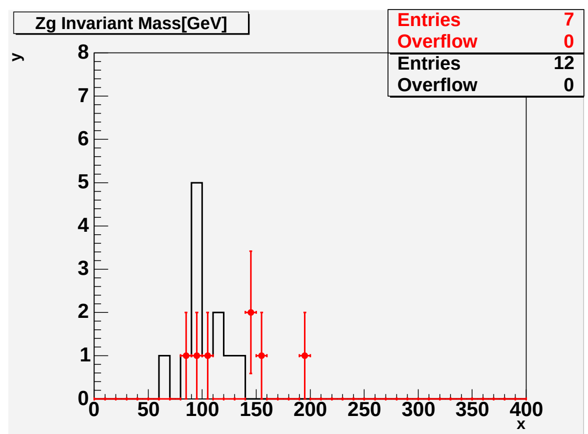

(d) $\ell\ell\gamma$ Invariant Mass

Figure 21: Multi-Lepton-Gamma Distributions: Muon Channel. Numbers of events in the first 305 pb^{-1} is shown in black, number of events in new $610pb^{-1}$ is shown in red.

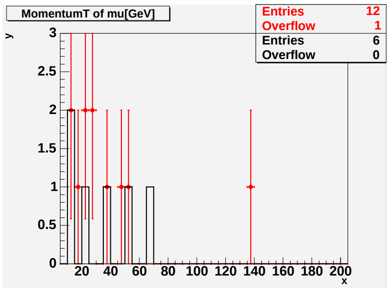

(a) Muon P_T

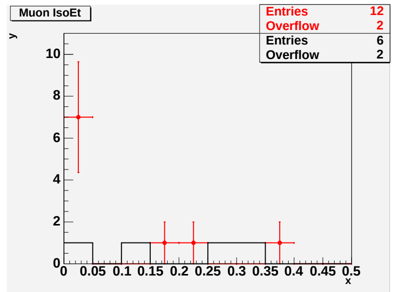

(b) Muon Iso E_T

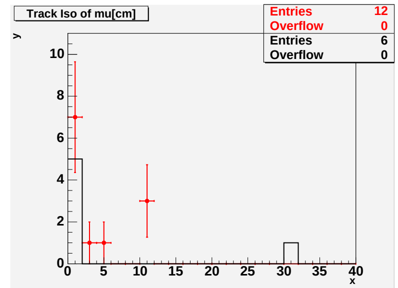

(c) Muon Track Iso

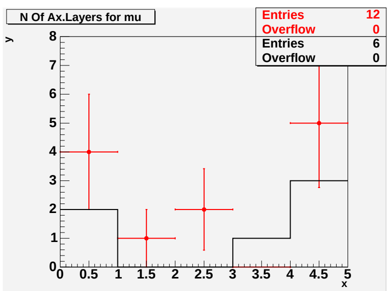

(d) Muon Axial COT hits

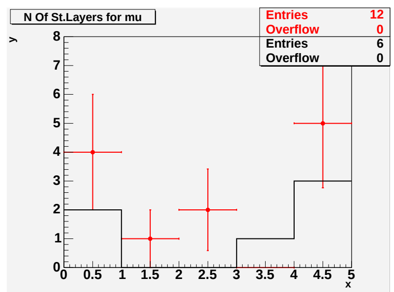

(e) Muon Stereo COT hits

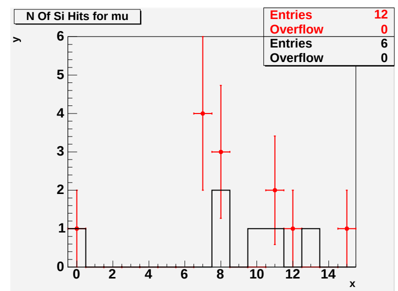

(f) Muon Si hits

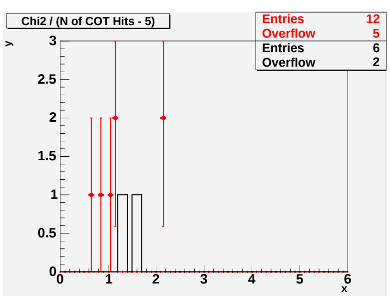

(g) Muon χ^2

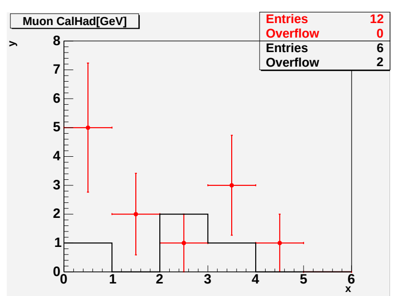

(h) Muon Cal HAD Energy

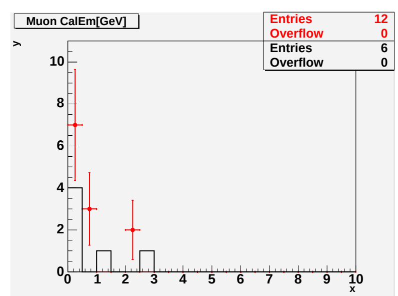

(i) Muon Cal EM Energy

Figure 22: Additional tracks in $\mu\gamma\not{E}_T$. Numbers of events in the first 305 pb^{-1} is shown in black, number of events in new $610 pb^{-1}$ is shown in red.

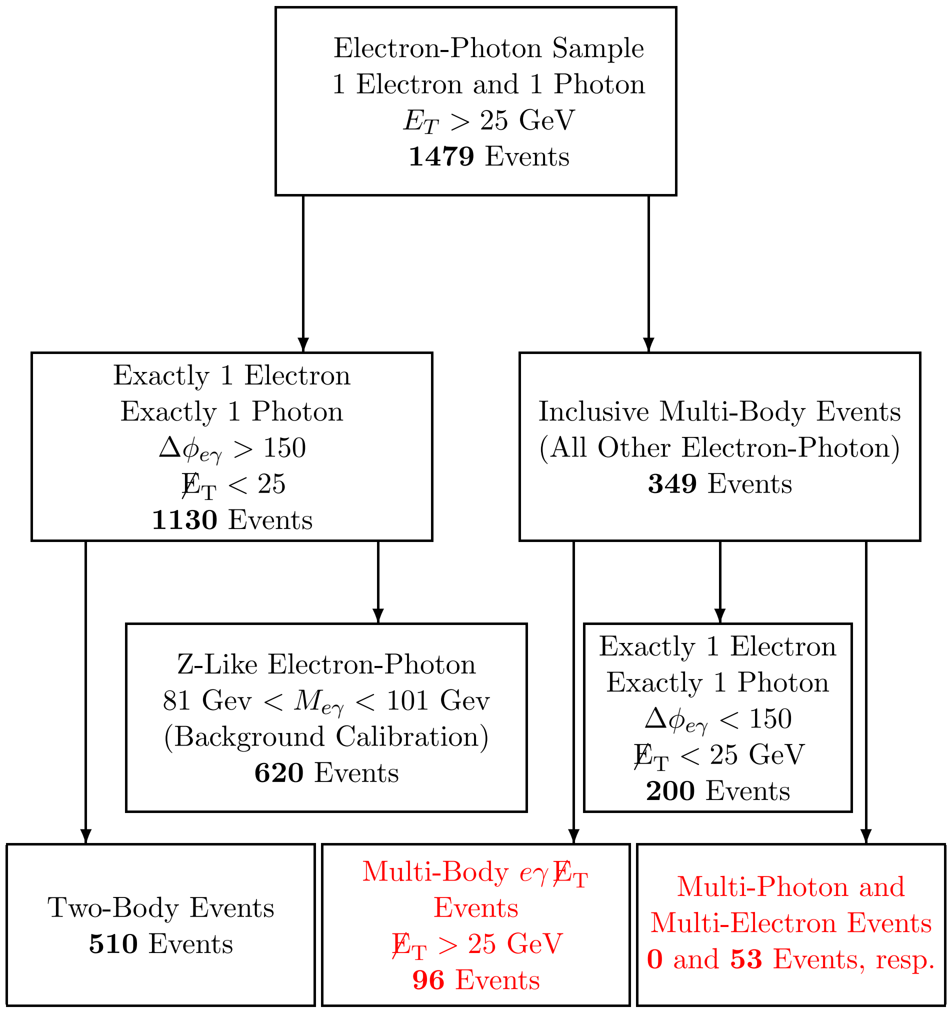

Figure 23: Electron-Photon Sample: the subsets of inclusive $e\gamma$ events analyzed in this paper

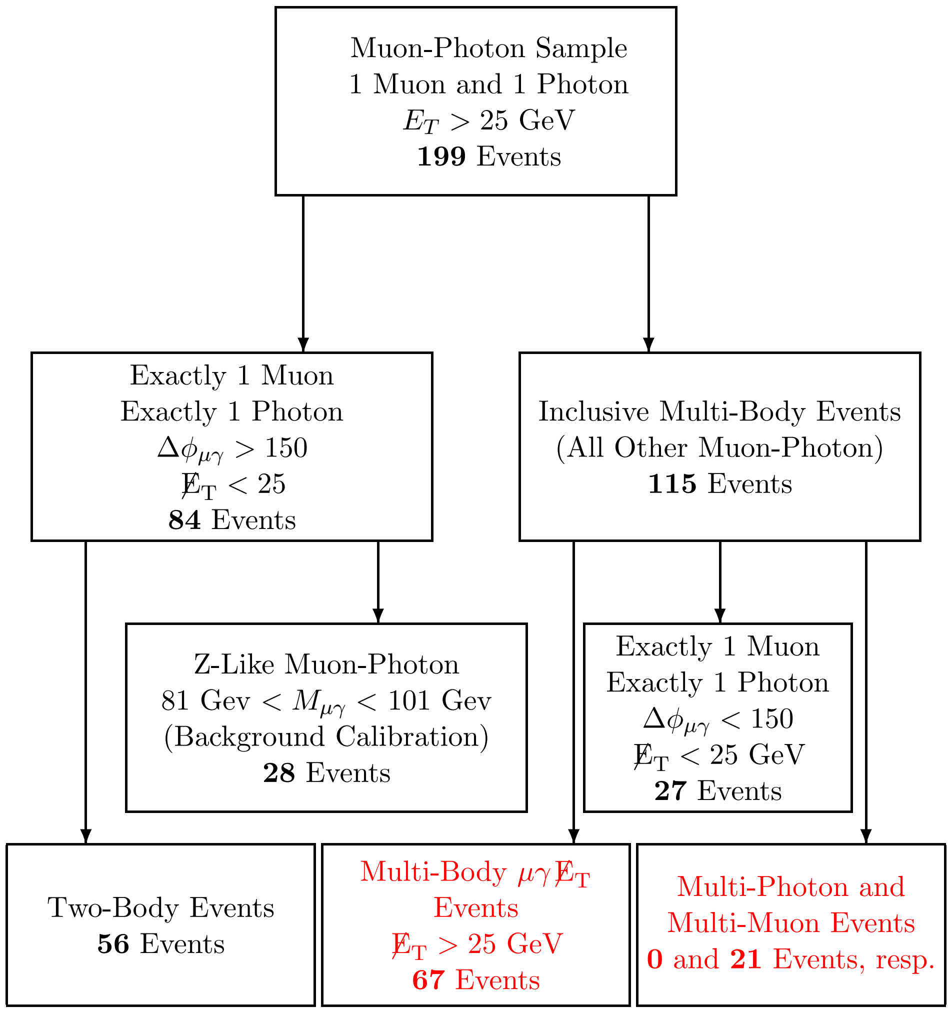

Figure 24: Muon-Photon Sample: the subsets of inclusive $\mu\gamma$ events analyzed in this paper

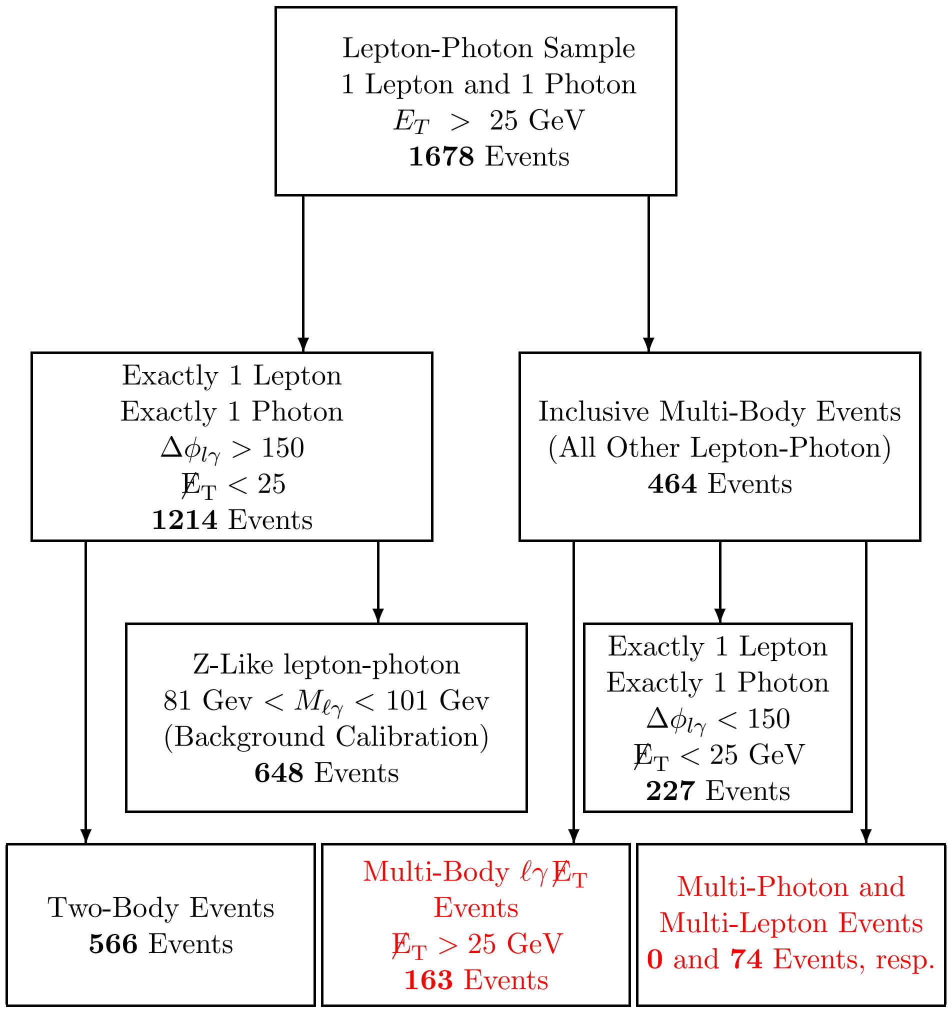

Figure 25: Lepton-Photon Sample: the subsets of inclusive $\ell\gamma$ events analyzed in this paper

C Comparison of Observed and Expected Numbers of Lepton-Photon Events

Shown further in the note are Tables and "Golden Plots" for the $\ell\gamma\not{E}_{\mathrm{T}}$ and $\ell\ell\gamma$ categories. You will find comments on the variables displayed on the plots below:

For the electron channel:

- Fiduciality is a fidEle variable, which can have following values:

  -1 error (null strip/wire cluster)

  0 not fiducial in central or plug

  1 fiducial in central or plug

  2 fiducial, but in CEM Tower 9

  3 fiducial, but in Chimney wedge tower 7

  4 fiducial in CEM using max pt track extrapolated to plane of CES

  5 fiducial in PEM using PES

  6 fiducial in PEM using max $\mathrm{P_T}$ track extrapolated to plane of PES

- H_T is a sum of E_T's P_T's of all objects in the event(leptons, photons, $\not{E}_{\mathrm{T}}$, jets) (Section **??**)
- Details on $\not{E}_{\mathrm{T}}$ can be found in Section **??**
- For $\Delta R(\ell\gamma)$ plot for Multi-Lepton-Gamma distributions we take ΔR between lepton and photon for both leptons

CDF Run II Preliminary, $929pb^{-1}$			
Lepton+ Gamma +$\not\!\!E_{\rm T}$ Events			
Standard Model Source	$e\gamma\not\!\!E_{\rm T}$	$\mu\gamma\not\!\!E_{\rm T}$	$(e+\mu)\gamma\not\!\!E_{\rm T}$
$W^{\pm}\gamma$	41.65 ± 4.84	29.85 ± 5.62	71.50 ± 10.01
$Z^0/\gamma + \gamma$	3.65 ± 1.31	14.10 ± 2.36	17.75 ± 3.65
$W^{\pm}\gamma\gamma$	0.32 ± 0.042	0.18 ± 0.025	0.50 ± 0.064
$Z^0/\gamma + \gamma\gamma$	0.087 ± 0.012	0.38 ± 0.048	0.47 ± 0.058
$t\bar{t}\gamma$	0.22 ± 0.029	0.13 ± 0.019	0.35 ± 0.045
$Z^0 \rightarrow e^+e^-, e \rightarrow \gamma$	9.59 ± 0.76	–	9.59 ± 0.76
Jet faking γ	21.5 ± 4.80	6.2 ± 3.60	27.7 ± 6.00
$\tau\gamma$ contribution	2.15 ± 0.56	0.76 ± 0.24	2.91 ± 0.65
QCD(Jets faking ℓ and $\not\!\!E_{\rm T}$)	15.0 ± 4.12	0.0 ± 0.100	15.0 ± 4.12
DIF (Decays-In-Flight)	–	2.3 ± 0.72	2.3 ± 0.72
Total	$94.17 \pm 4.71(stat)$ $\pm 6.64(sys)$	$53.90 \pm 1.94(stat)$ $\pm 6.84(sys)$	$148.07 \pm 5.10(stat)$ $\pm 11.93(sys)$
	$94.17 \pm 8.14(tot)$	$53.90 \pm 7.11(tot)$	$148.07 \pm 12.97(tot)$
Observed in Data	96	67	163

Table 9: The predicted number of lepton-photon-$\not\!\!E_{\rm T}$ events in $929pb^{-1}$ from Standard Model sources, and the numbers of events observed. **Backgrounds from misidentifies muons ("Decays-in-flight") are not included.**

CDF Run II Preliminary, $929pb^{-1}$			
Multi-Photon + Lepton Predicted Events			
SM Source	$e\gamma\gamma$	$\mu\gamma\gamma$	$\ell\gamma\gamma$
$Z^0\gamma$	37.85 ± 4.65	25.55 ± 2.88	63.40 ± 7.48
$Z^0\gamma\gamma$	0.72 ± 0.088	0.40 ± 0.050	1.12 ± 0.13
Z^0+Jet, jet faking γ	0.0 ± 1.20	0.0 ± 1.10	0.0 ± 1.60
$Z^0 \rightarrow e^+e^-, e \rightarrow \gamma$	0.38 ± 0.11	–	0.38 ± 0.11
QCD (Non-WZ) fakes	0.0 ± 0.20	0.0 ± 0.100	0.0 ± 0.20
DIF (Decays-In-Flight)	–	0.0 ± 0.20	0.0 ± 0.20
Total	$38.95 \pm 0.71(stat)$ $\pm 4.75(sys)$	$25.95 \pm 0.56(stat)$ $\pm 3.04(sys)$	$64.93 \pm 0.89(stat)$ $\pm 7.60(sys)$
	$38.95 \pm 4.80(tot)$	$25.95 \pm 3.09(tot)$	$64.93 \pm 7.65(tot)$
Observed	53	21	74

Table 10: The predicted number of multi-body events with additional leptons in $929pb^{-1}$ from Standard Model sources, and the numbers of events observed. The Z^0+Jet and $W\gamma$+Jet predictions are taken from the data.

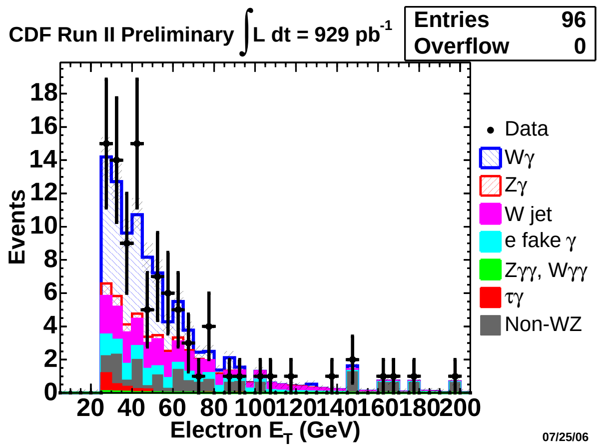

(a) Electron E_T

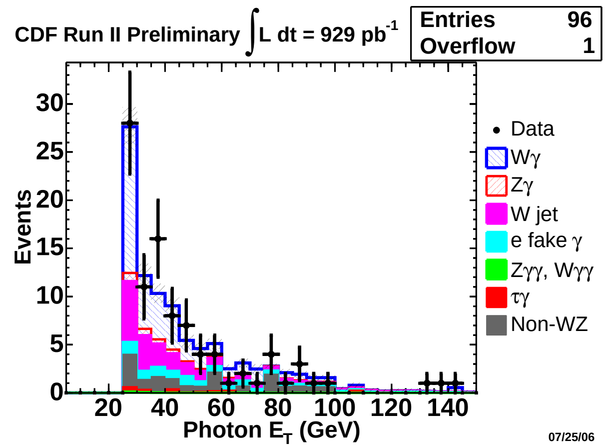

(b) Photon E_T

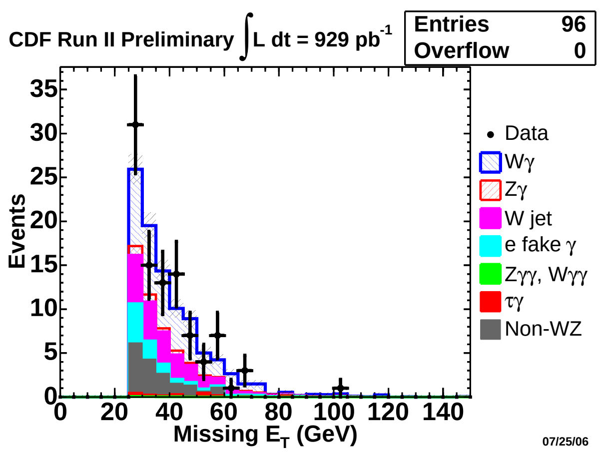

(c) $\not\!\!E_T$

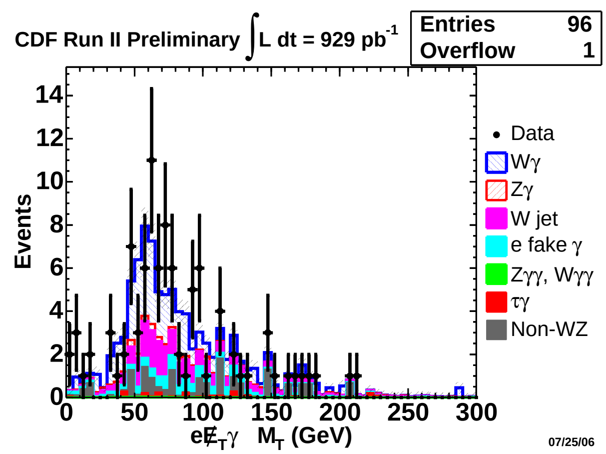

(d) $e\gamma\not\!\!E_T$ Transverse Mass

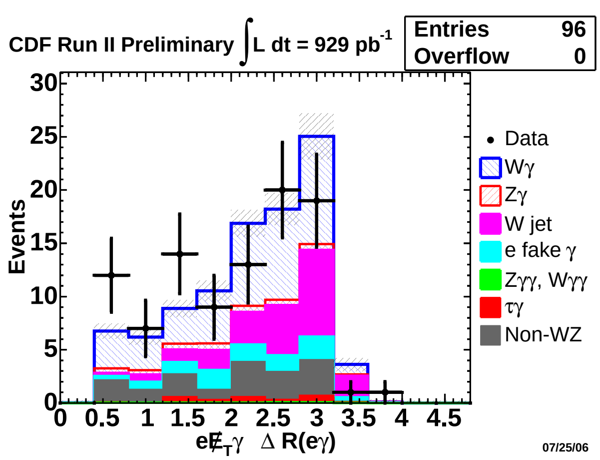

(e) $\Delta R(e\gamma)$

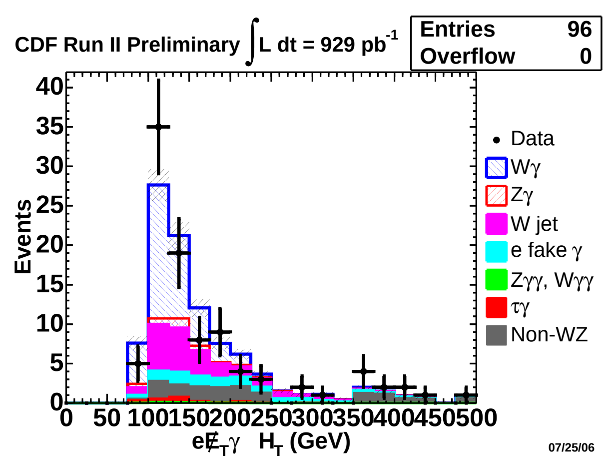

(f) H_T for $e\gamma\not\!\!E_T$ Candidate Events

Figure 26: Lepton-Gamma-Met Distributions#1: Electron Channel

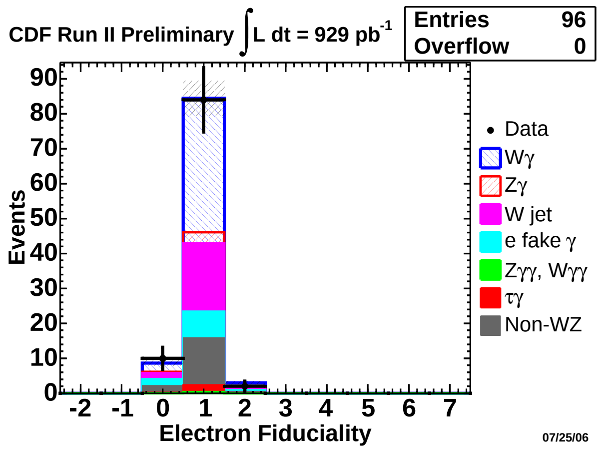

(a) Electron Fiduciality

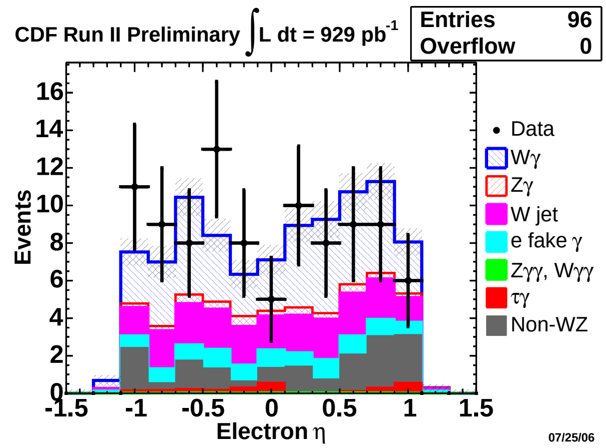

(b) Electron η

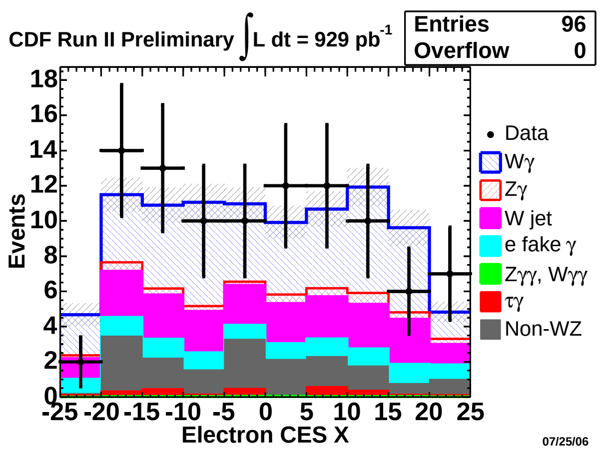

(c) Electron CES X

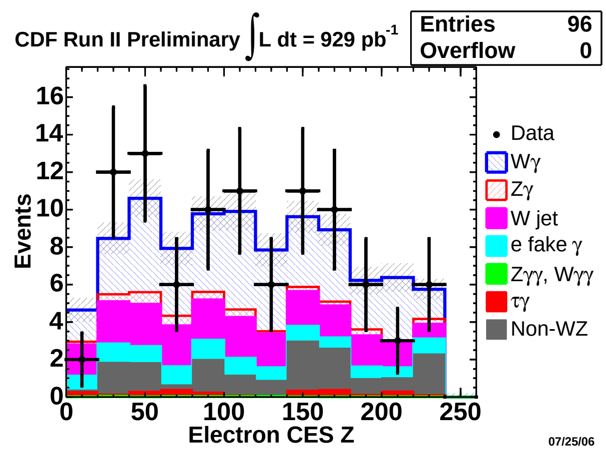

(d) Electron CES Z

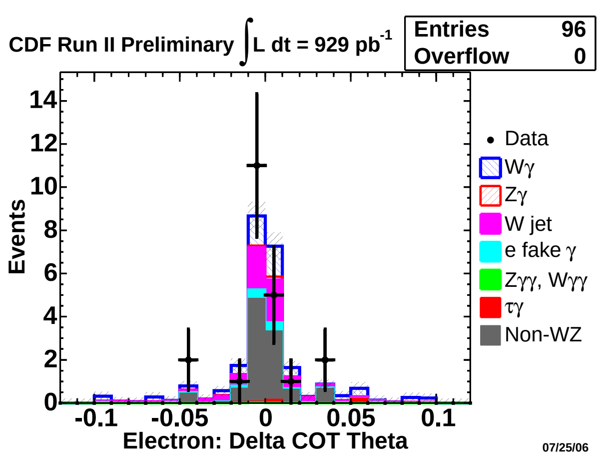

(e) Electron: Delta COT Theta

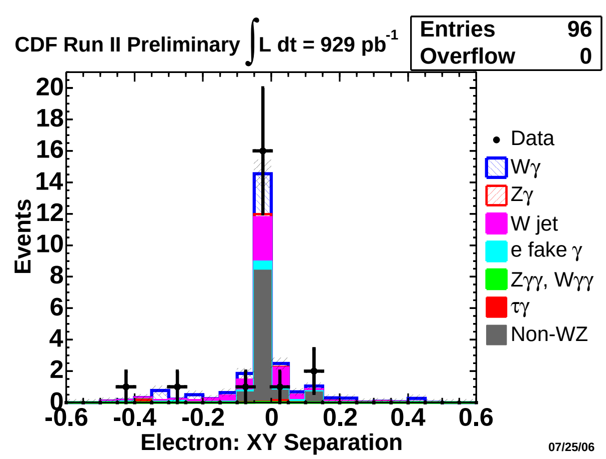

(f) Electron: XY Separation

Figure 27: Lepton-Gamma-Met Distributions#2: Electron Channel. There is only one trident in the $e\gamma\not{E}_T$ sample.

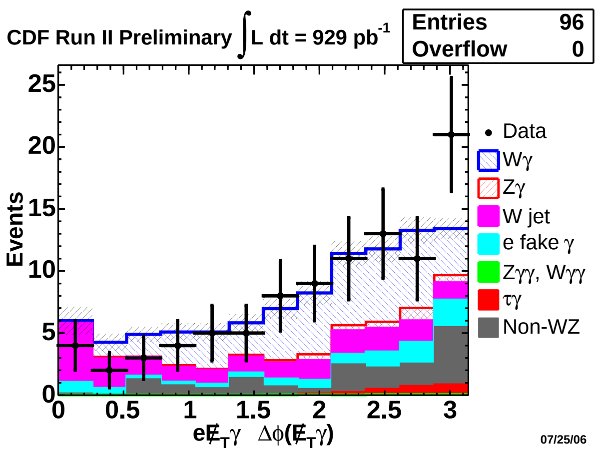

(a) $\Delta\phi(\gamma \not\!\!E_{\mathrm{T}})$

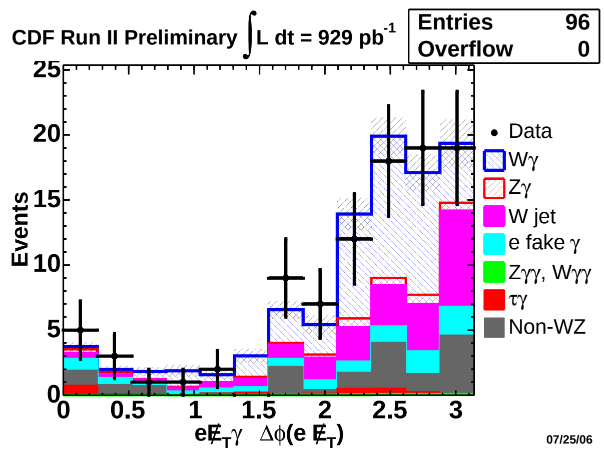

(b) $\Delta\phi(e \not\!\!E_{\mathrm{T}})$

Figure 28: Lepton-Gamma-Met Distributions#3: Electron Channel.

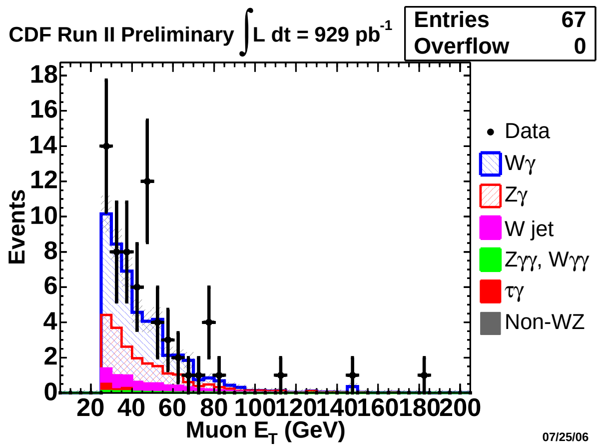

(a) Muon P_T

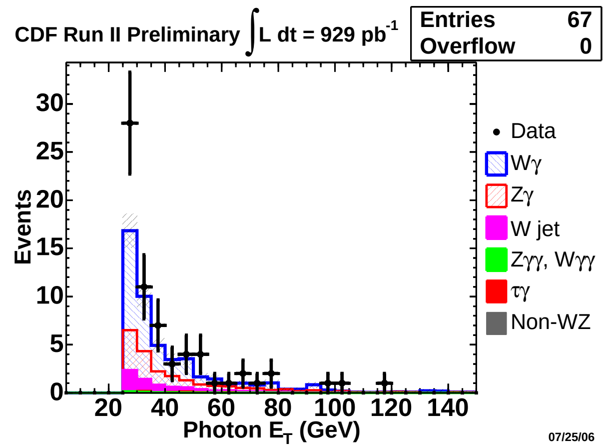

(b) Photon E_T

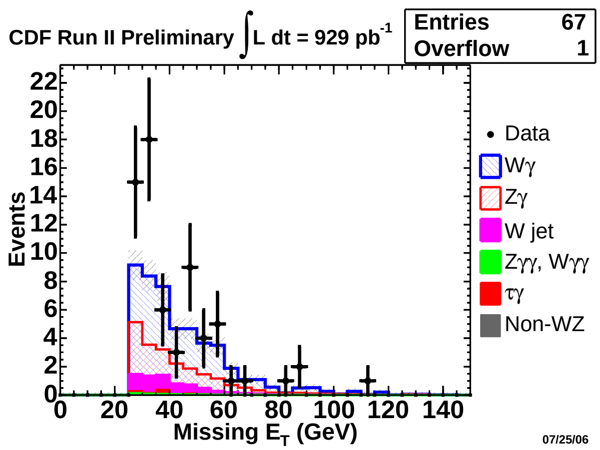

(c) $\not\!\!E_T$

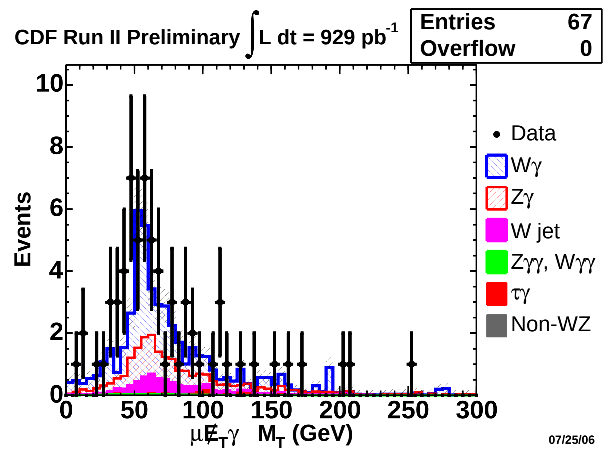

(d) $\mu\gamma\not\!\!E_T$ Transverse Mass

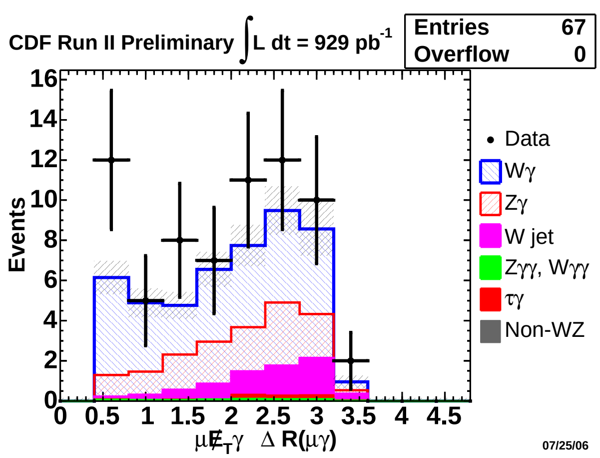

(e) $\Delta R(\mu\gamma)$

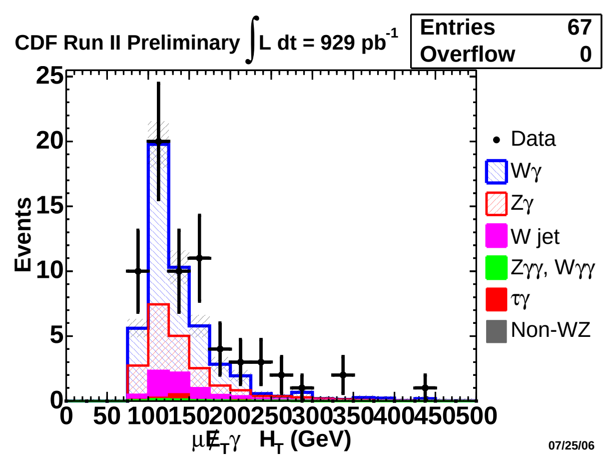

(f) H_T for $\mu\gamma\not\!\!E_T$ Candidate Events

Figure 29: Lepton-Gamma-Met Distributions#1: Muon Channel

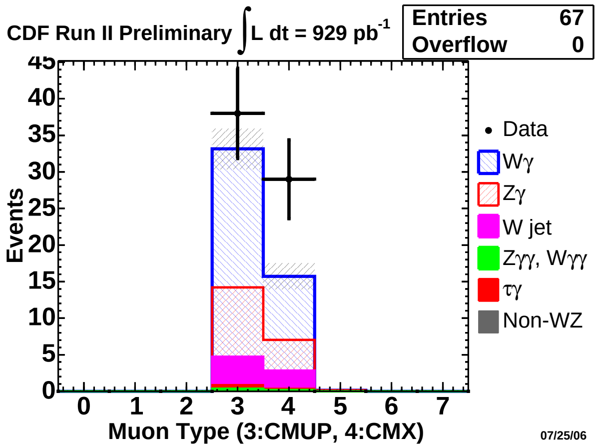

(a) Muon Detector Type

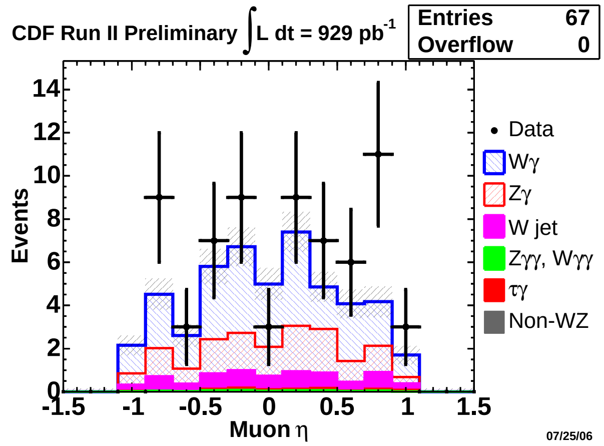

(b) Muon η

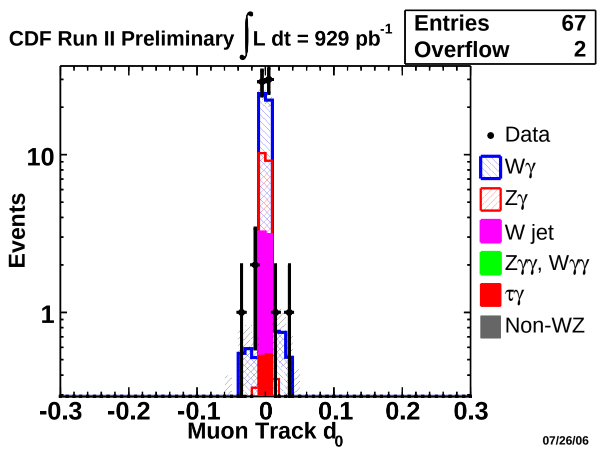

(c) Muon Track d_0

Figure 30: Lepton-Gamma-Met Distributions#2: Muon Channel

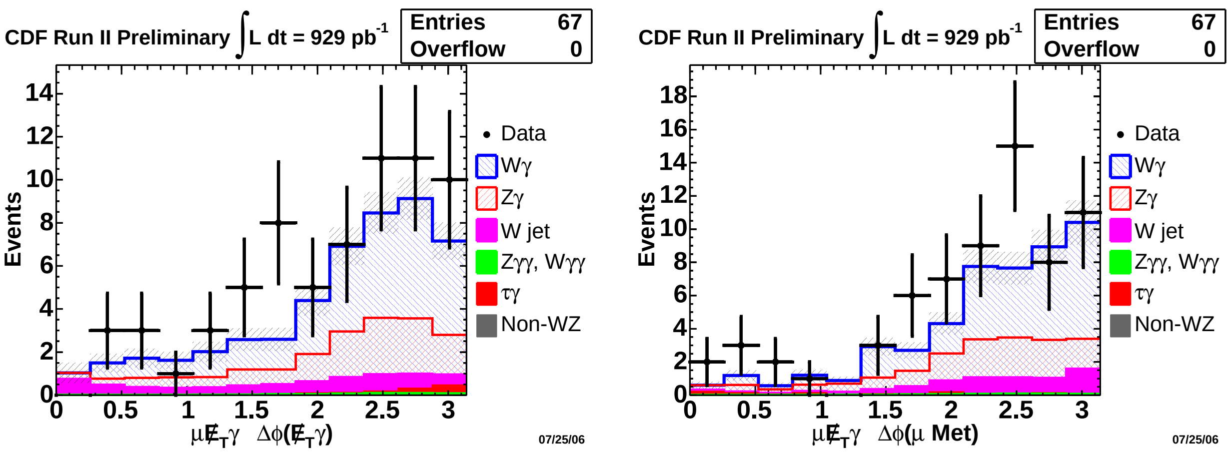

(a) $\Delta\phi(\gamma \not{E}_{\mathrm{T}})$

(b) $\Delta\phi(\mu \not{E}_{\mathrm{T}})$

Figure 31: Lepton-Gamma-Met Distributions#3: Muon Channel.

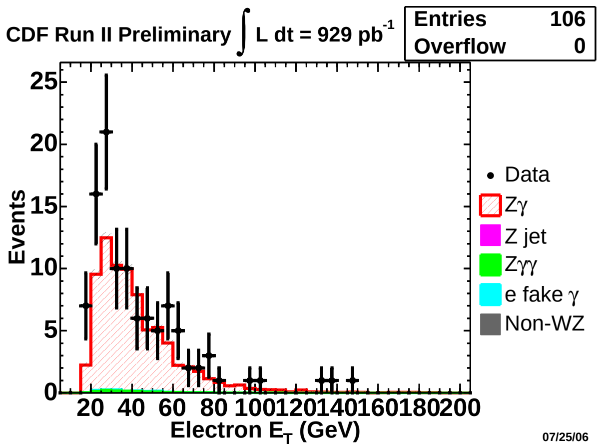

(a) Electron E_T

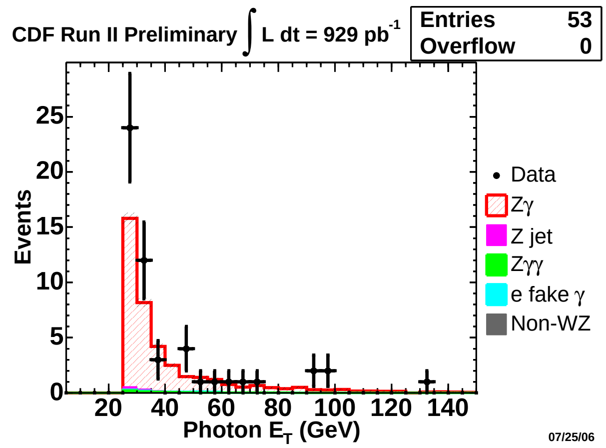

(b) Photon E_T

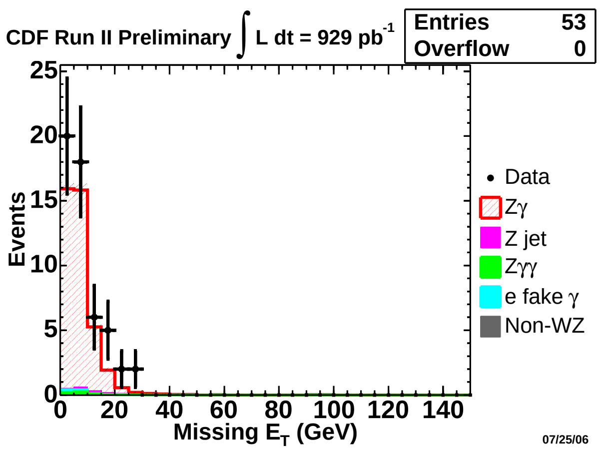

(c) $\not{E}_{\mathrm{T}}$

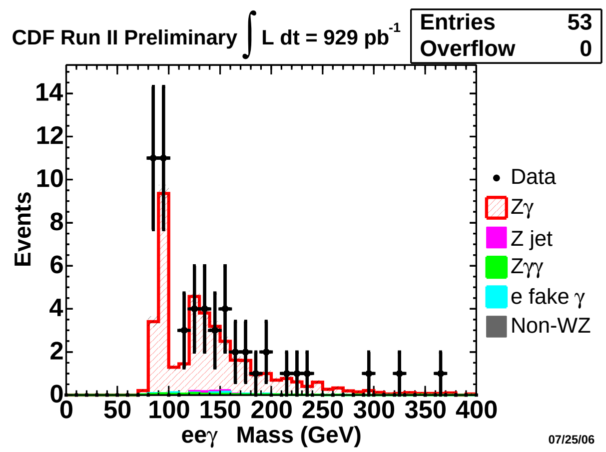

(d) $ee\gamma$ Invariant Mass

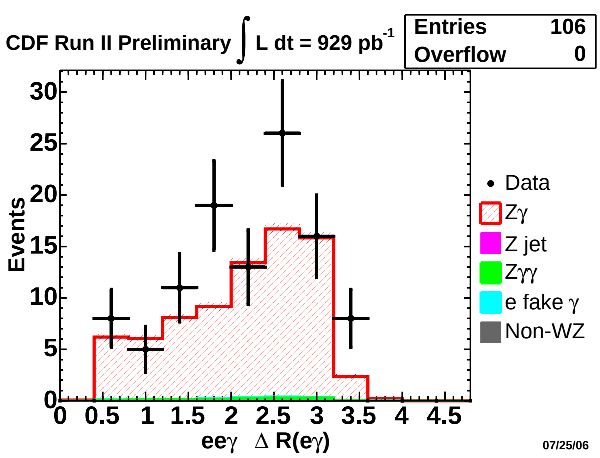

(e) $\Delta R(e\gamma)$, for both electrons

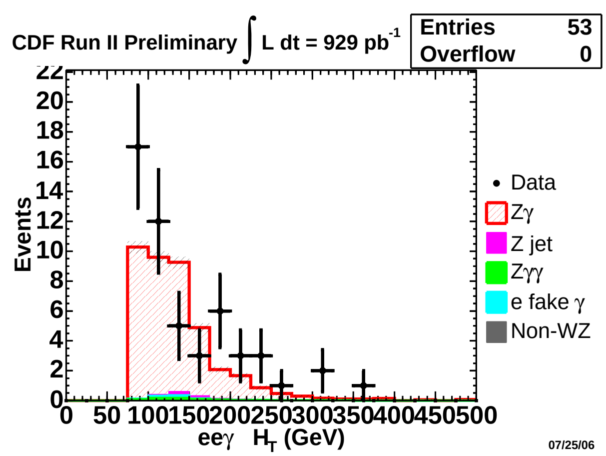

(f) H_T for $ee\gamma$ Candidate Events

Figure 32: Multi-Lepton-Gamma Distributions: Electron Channel.

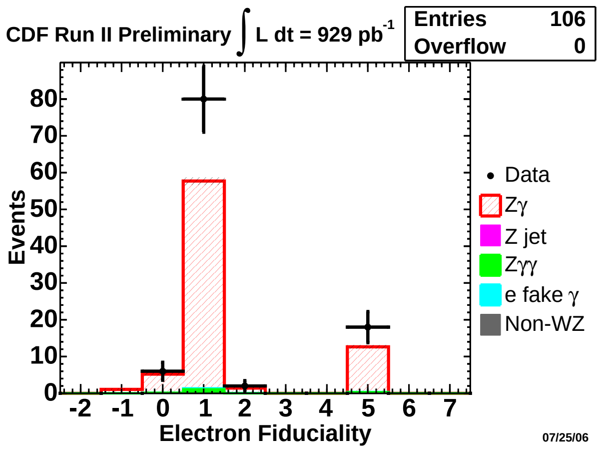

(a) Electron Fiduciality

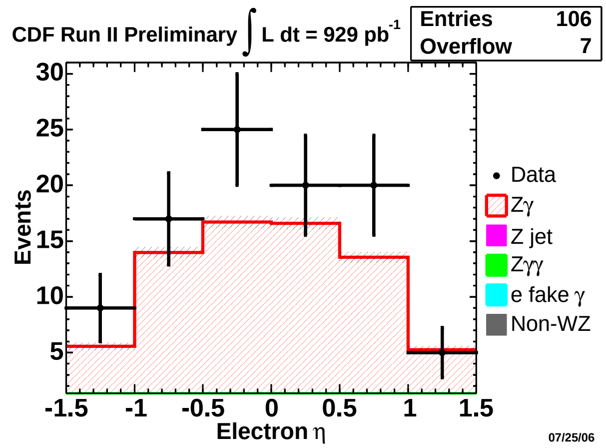

(b) Electron η

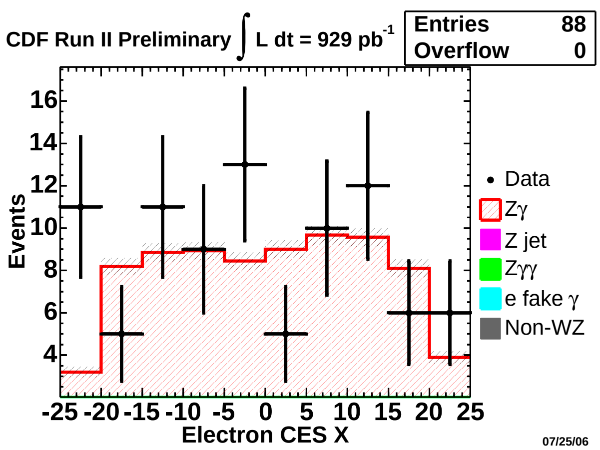

(c) Electron CES X

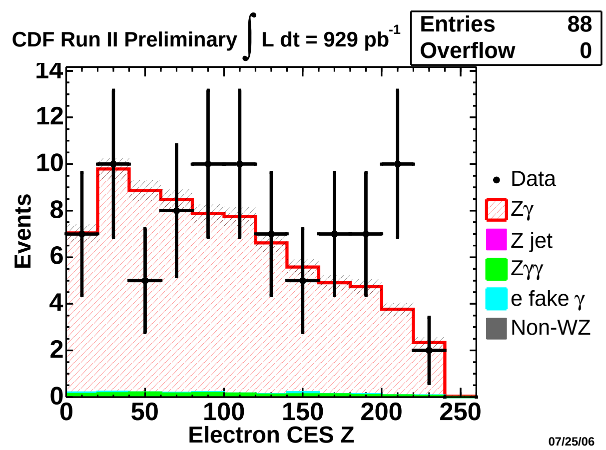

(d) Electron CES Z

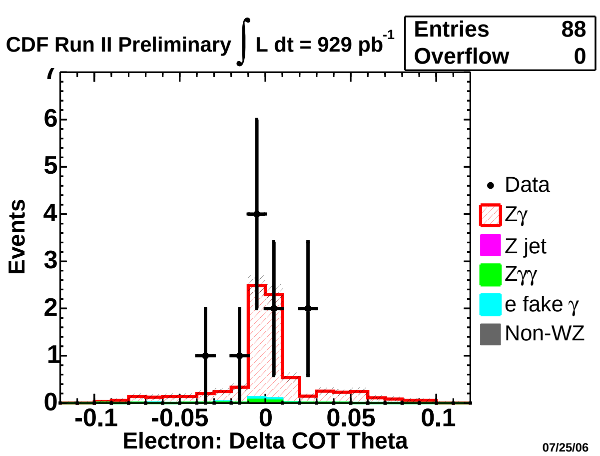

(e) Electron: Delta COT Theta

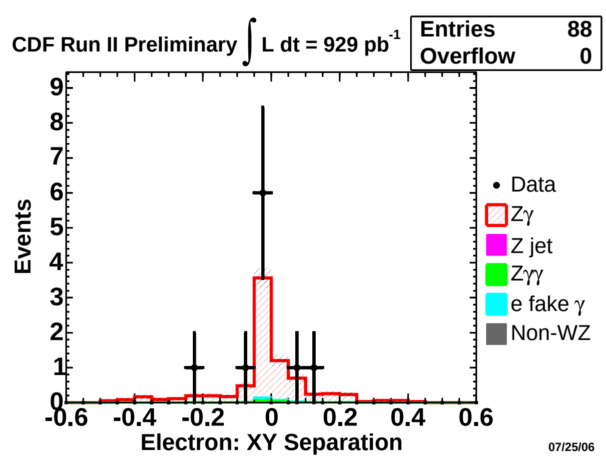

(f) Electron: XY Separation

Figure 33: Multi-Lepton-Gamma Distributions#2: Electron Channel. There is one conversion electron and two tridents in the $ee\gamma$ sample.

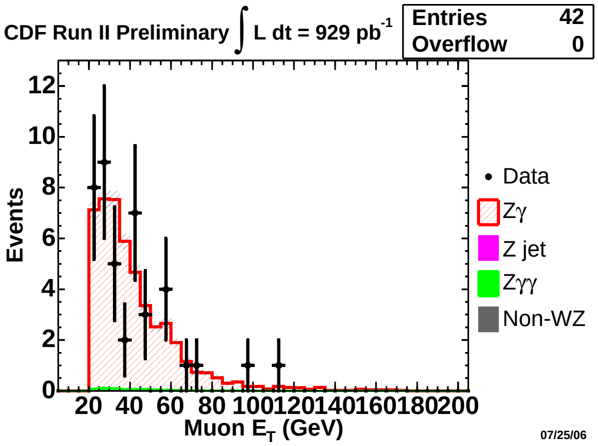

(a) Muon P_T

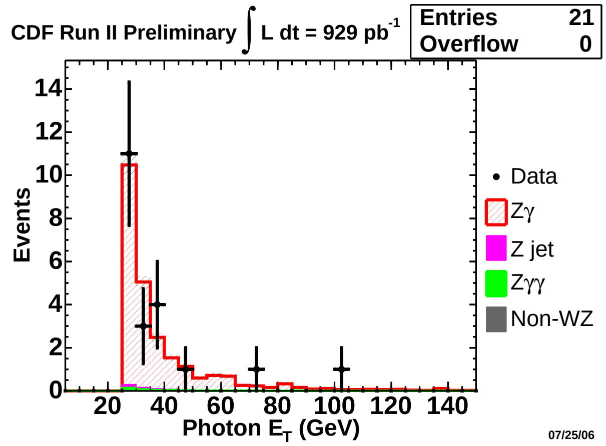

(b) Photon E_T

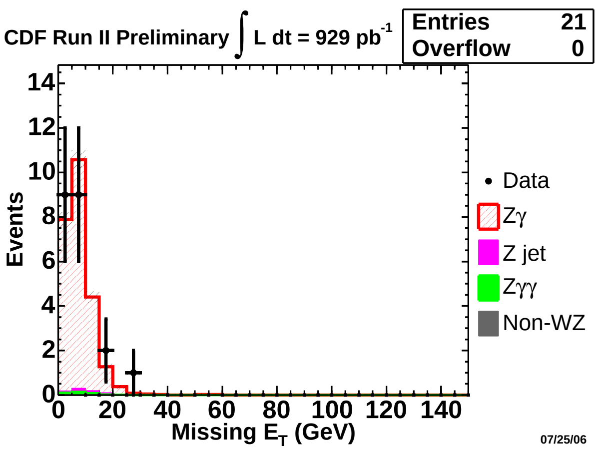

(c) $\not\!\!E_T$

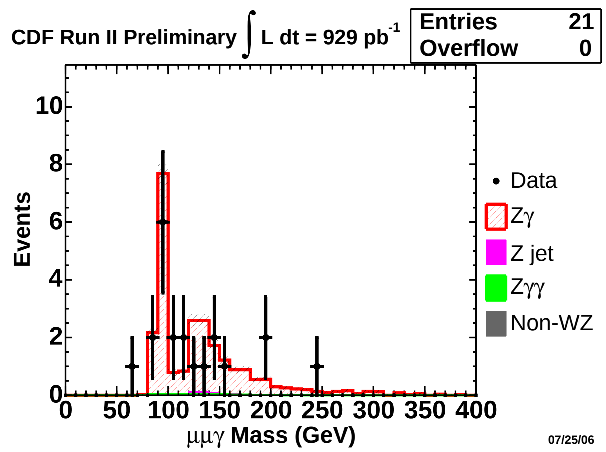

(d) $\mu\mu\gamma$ Invariant Mass

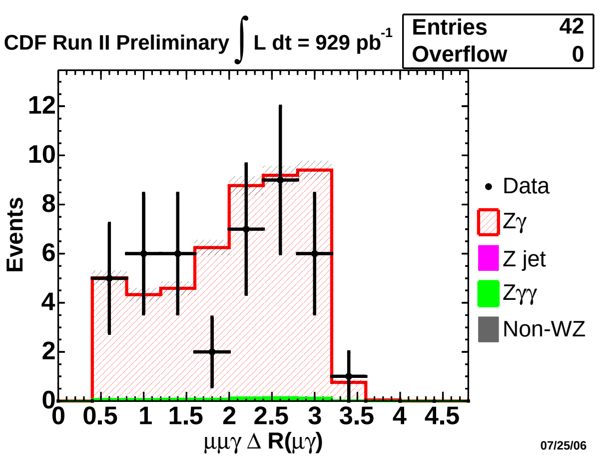

(e) $\Delta R(\mu\gamma)$, for both muons

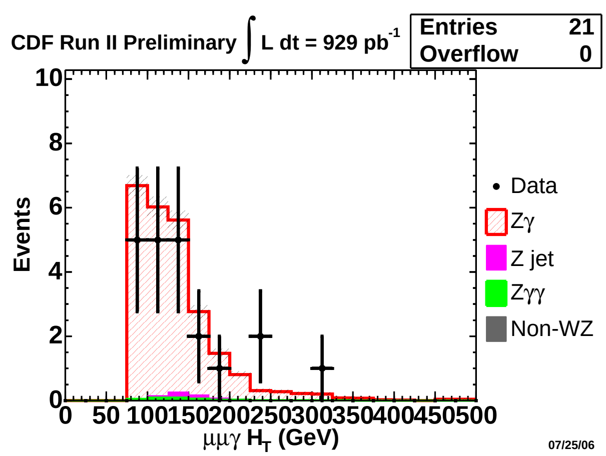

(f) H_T for $\mu\mu\gamma$ Candidate Events

Figure 34: Multi-Lepton-Gamma Distributions: Muon Channel

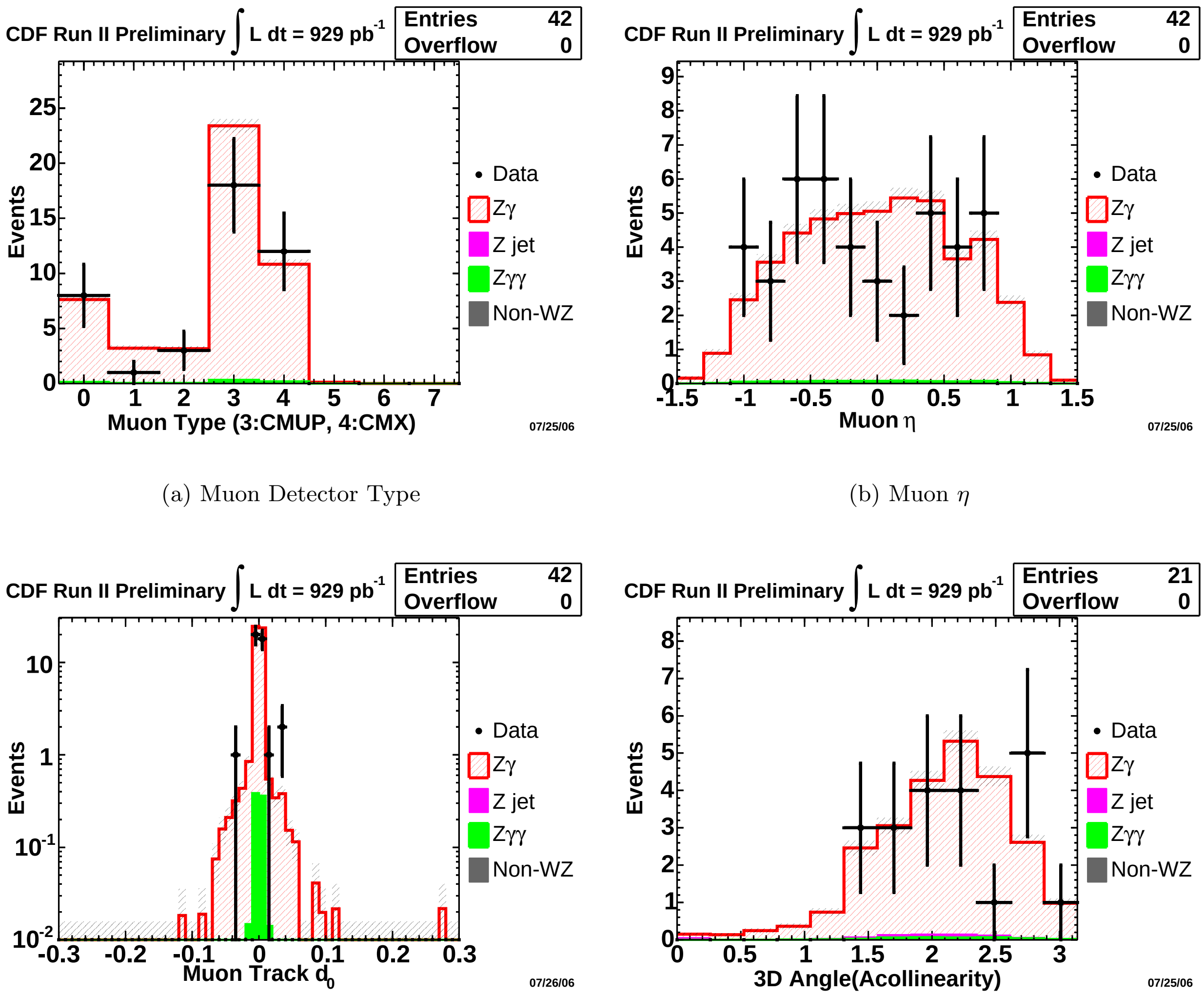

(a) Muon Detector Type

(b) Muon η

(c) Muon Track d_0

(d) Muon Acollinearity (3D Angle($\mu\mu$))

Figure 35: Multi-Lepton-Gamma Distributions#2: Muon Channel

C.1 Extra plots for the muons from the $\mu\mu\gamma$

We've made some additional DATA vs MC plots to check ID variables for the muons from the $\mu\mu\gamma$ events.

Iso E_T is a relative calorimeter isolation (calorimeter isolation/calorimeter energy).

Iso P_T is a relative track isolation (track isolation/track pt).

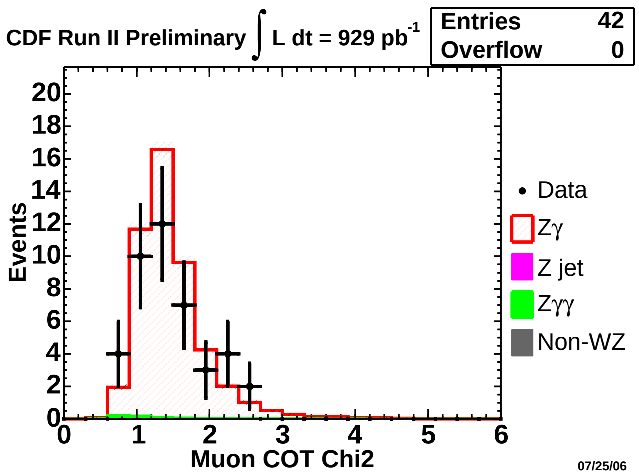

(a) Muon Chi2

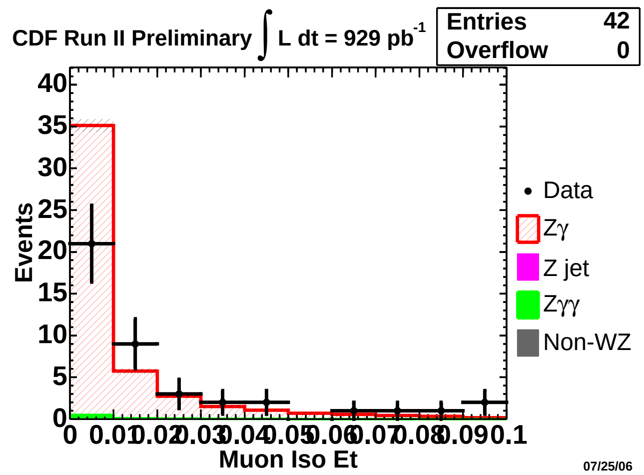

(b) Muon Iso E_T

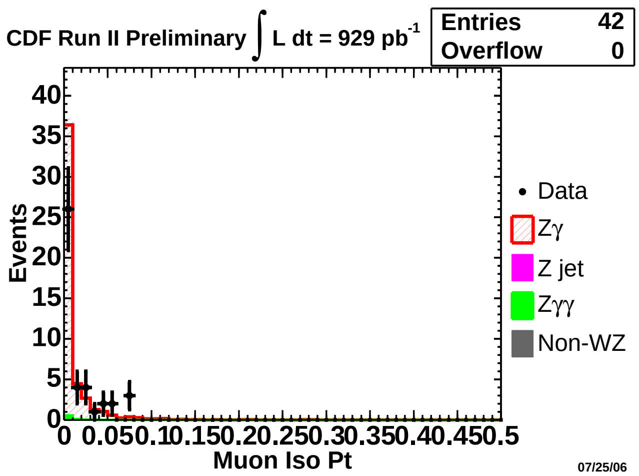

(c) Muon Iso P_T

Figure 36: Multi-Lepton-Gamma Distributions: Muon Channel

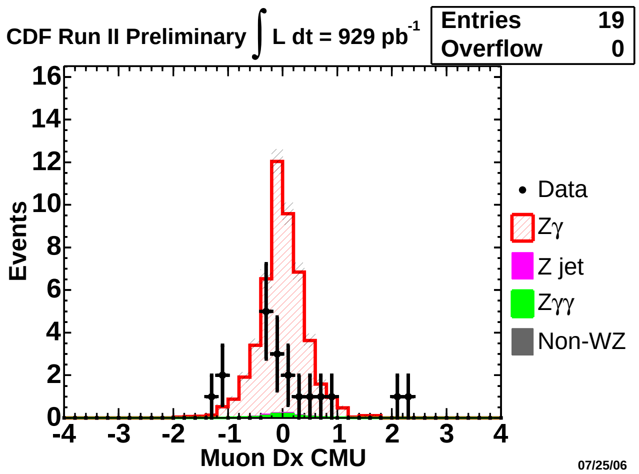

(a) Muon ΔX CMU

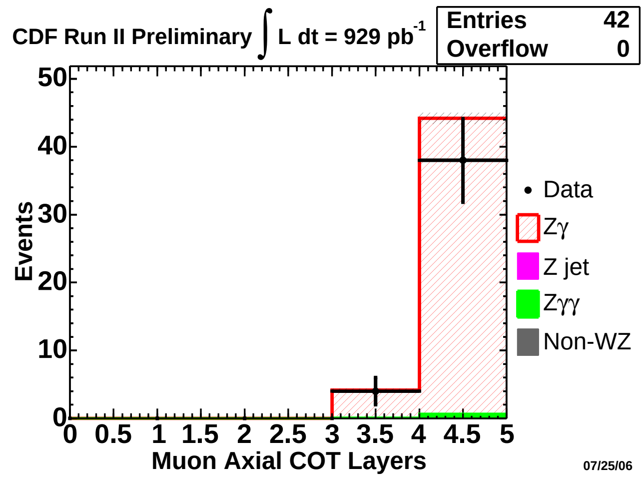

(b) Muon N Axial Segments

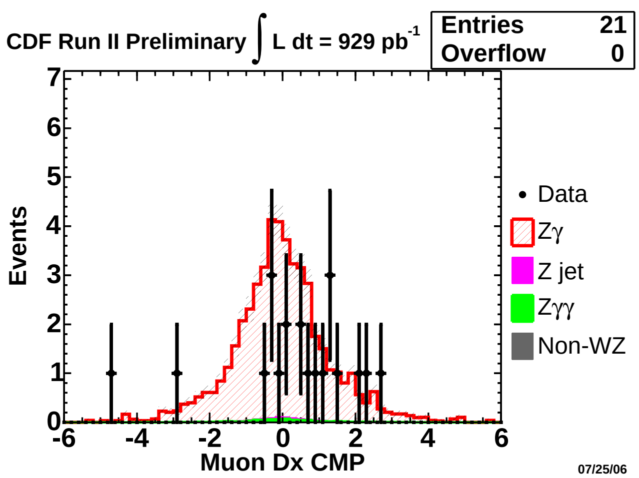

(c) Muon ΔX CMP

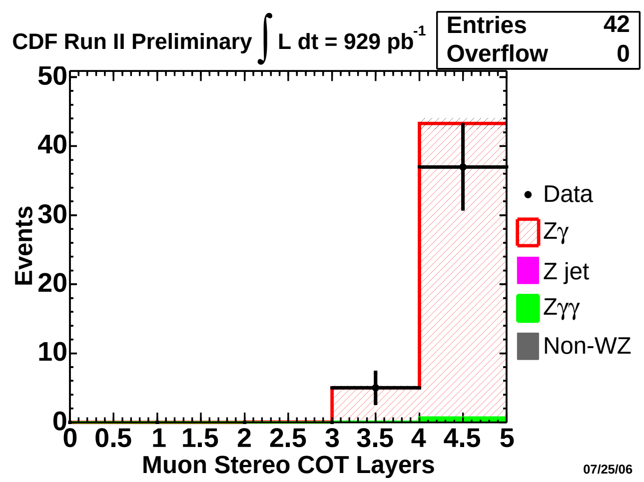

(d) Muon N Stereo Segments

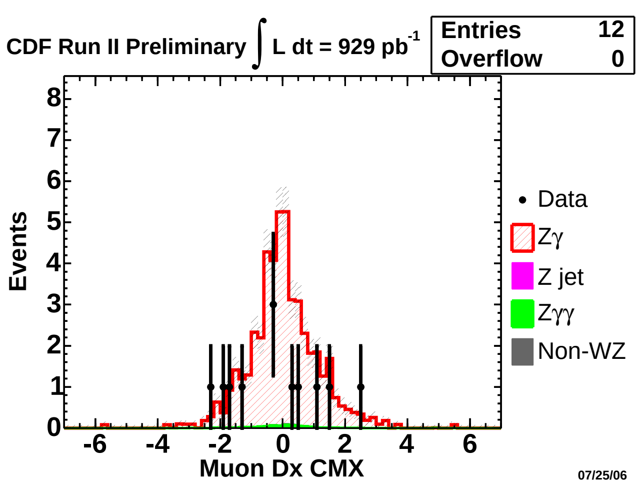

(e) Muon ΔX CMX

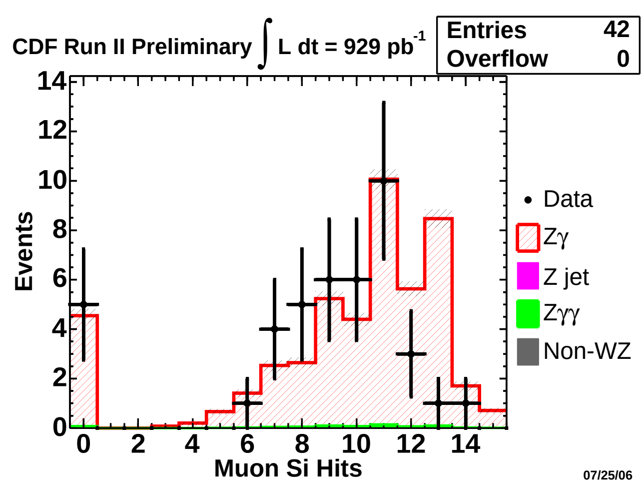

(f) Muon N Si Hits

Figure 37: Multi-Lepton-Gamma Distributions: Muon Channel

References

[1] A. Abulencia *et al.* (CDF Collaboration). Search for New Physics in Lepton + Photon + X Events with 305 pb^{-1} of p$\bar{\text{p}}$ Collisions at $\sqrt{s}$= 1.96 TeV. *Submitted to Phys.Rev.Lett.; FERMILAB-PUB-06-127-E; hep-ex 0605097*, 2006.

[2] Henry Frisch, Andrei Loginov. Search for lepton-photon +x events in 300 pb^{-1}. CDF Note 7550, CDF, 2005.

[3] P. Onyisi and the UC CDF Physics Group. The ucntuple is described on the web page:. http://hep.uchicago.edu/cdf/flatntuple, 2004.

[4] UC CDF Physics Group. The ucntuple sets are listed on the web page:. http://hep.uchicago.edu/cdf/datasets/, 2004.

[5] H.Frisch, A.Loginov, S.Tsuno. $W\gamma$ and $Z\gamma$ MC MadGraph and Baur Samples. CDF Note 8116, CDF, 2006.

[6] R.Culbertson, R.Field, H.Frisch, A.Goshaw, B.Heinemann, M.Kirby, A.Loginov, S.Mrenna, P.Murat, S.Tsuno, Un-Ki Yang. Pythia Settings for Generating $W\gamma$, $Z\gamma$, $W\gamma\gamma$, $Z\gamma\gamma$ Monte Carlo. SM Matching. CDF Note 8126, CDF, 2006.

[7] Irina Shreyber, Andrei Loginov, Henry Frisch. Search for $\ell\gamma \not{E}_{\mathrm{T}} b$ + x ($t\bar{t} + \gamma$) events. CDF Note TTBAR (to be published), CDF, 2006.

[8] D. Acosta *et al.* Measurement of W gamma and Z gamma Production in p anti-p Collisions at s**(1/2) = 1.96 TeV. *Phys. Rev. Lett. 94, 041803 (2005)*, 2005.

[9] T. Stelzer and W. F. Long, Comput. Phys. Commun. **81**, 357 (1994); F. Maltoni and T. Stelzer, JHEP **302**, 27 (2003); hep-ph/0208156. We designate the production of lepton pairs through the Drell-Yan process, including both the Z^0 and γ amplitudes, as Z^0/γ^* in signatures such as $\bar{p}p \to Z^0/\gamma^* + \gamma \to e^+e^-\gamma$. We use version v3.2.

[10] U. Baur, T. Han, and J. Ohnemus, Phys. Rev. D **48**, 5140 (1993); J. Ohnemus, Phys. Rev. D **47**, 940 (1993).

[11] A. Pukhov, E. Boos, M. Dubinin and others. Comphep: A package for evaluation of Feynman diagrams and integration over multiparticle phase space. By A. Pukhov, E. Boos, M. Dubinin, V. Edneral, V. Ilyin, D. Kovalenko, A. Kryukov, V. Savrin (Moscow State U.), S. Shichanin (Serpukhov, IHEP), A. Semenov (Dubna, JINR). INP-MSU-98-41-542, Aug 1999. 126pp. User's manual for version 33. e-Print Archive: hep-ph/9908288; E.E. Boos, M.N. Dubinin, V.A. Ilyin, A.E. Pukhov, and V.I. Savrin, INP MSU 94-36/358 and SNUTP-94-116, hep-ph/9503280; P. Baikov *et al.*, in Proc. of the Xth Int. Workshop on High Energy Physics and Quantum Field Theory, QFTHEP-95, ed. by B. Levtchenko and V. Savrin, (Moscow, 1995), p. 101. We use v4.1.10.

[12] See, for example, S. Ambrosanio, G.L. Kane, G.D. Kribs, S.P. Martin, and S. Mrenna, Phys. Rev. D **55**, 1372 (1997); B.C. Allanach, S. Lola, K. Sridhar, Phys. Rev. Lett. **89**, 011801 (2002); hep-ph/0111014.

[13] Kenichi Hatakeyama. Personal Communication.